

Sorbonne Université

2021-2022

Stage de Master 2

Noé Bassel

Titre

Projet réalisé en collaboration avec le CERMICS
Ecole Nationale des Ponts et Chaussées
6 et 8 avenue Blaise Pascal
Cité Descartes - Champs sur Marne
77455 Marne la Vallée Cedex 2

Tuteur : Gabriel Stoltz

May 23, 2022

Contents

1	Introduction to molecular dynamics	4
1.1	The microscopic description of atomic systems	4
1.1.1	Classical phase space	4
1.1.2	Dynamical description	5
1.1.3	Reduced units	6
1.2	Statistical ensembles	7
1.2.1	Microcanonical ensemble	8
1.2.2	Canonical ensemble	8
1.2.3	From microscopic dynamics to macroscopic observables	10
1.2.4	Examples of instantaneous observables	10
1.2.5	Ergodic averages	11
2	Sampling equilibrium ensembles	12
2.1	Properties of Hamiltonian dynamics	12
2.2	Microcanonical averages	12
2.2.1	Numerical schemes for Hamiltonian dynamics	14
2.2.2	Properties of symplectic schemes	15
2.2.3	Shortcomings of the Hamiltonian approach	16
2.3	Canonical averages	16
2.3.1	Langevin dynamics	16
2.3.2	Properties of the Langevin dynamics	17
2.3.3	Overdamped limit of Langevin dynamics	18
2.3.4	Splitting schemes for the Langevin dynamics	20
2.3.5	Error analysis for splitting schemes	21
2.3.6	Unbiased sampling	21
2.3.7	Asymptotic variance	23
2.3.8	Illustration: the equation of state of Argon	25
3	Transport coefficients	26
3.1	Non-equilibrium dynamics	26
3.2	Linear response theory	26
3.3	Numerical schemes	26
4	A Norton method	27
4.1	Introduction	27
4.2	Norton dynamics for the mobility observable	27
4.2.1	The dynamics	27
4.2.2	Analytic calculations for the kinetic dynamics	28
4.3	Splitting schemes	30
4.4	Estimating transport coefficients	30
A	Implementation details	31

B Study of the BAOA scheme	32
B.0.1 Definitions and notations	32
B.0.2 Relating invariant measures of discretization schemes	33
B.0.3 Error estimate on the phase space measure	35
B.0.4 Error estimates on the kinetic marginal distributions	36
B.0.5 Analysis of the second order error term for kinetic averages under $\mu_{\Delta t, P}$	37
B.0.6 Analysis of the discrepancy between the dominant error terms on the kinetic marginals.	39
B.1 Numerical results	40
B.1.1 Models	41
B.1.2 Equality of marginal configurational distributions	41
B.1.3 Comparison of marginal kinetic distributions	43
B.1.4 Verification of the first-order expansion	43
B.1.5 Example of first-order bias in a BAOA average	45
B.1.6 Effect of the friction parameter	46
C Notational conventions	47

Chapter 1

Introduction to molecular dynamics

1.1 The microscopic description of atomic systems

Molecular dynamics, and computational statistical physics at large, aim at simulating on the computer the behavior of physical systems. The hope is that one can infer quantities and properties of real-life interest from observing the results of numerical simulations, which may be relevant to understand the material properties of many-particle systems, or the nature of interactions in complex systems such as those found in biology. Computational simulations can thus act as surrogate experiments in cases where experimental setups are hard to achieve, or measurements are impossible. They can also be seen as surrogate tests of theoretical models, as they allow to test the validity of a mathematical description by comparing numerical predictions to experimental data. Molecular dynamics, in particular, is concerned with simulating atomic systems, most often (and as we shall systematically do) using a classical description.

1.1.1 Classical phase space

We consider a system of N particles evolving in d -dimensional space. The classical description contends that the *state* of a system is the datum of the positions and momenta of every particle in the system. We can interpret this as the statement that, given full knowledge of the positions and momenta at some initial time, and of the forces at play, one can deduce exactly the positions and momenta at any future time. It is often the case in computer simulations that we consider positions which are restricted to a bounded domain by the use of periodic boundary conditions. To that effect, let

$$\mathcal{D} = (LT)^{dN} \text{ or } \mathbb{R}^{dN},$$

where \mathbb{T} is the one-dimensional torus. We call \mathcal{D} the configuration space.

Definition 1 (Phase space). *We describe the positions and momenta of the atoms as vectors*

$$q = (q_{1,1}, \dots, q_{1,d}, \dots, q_{N,1}, \dots, q_{N,d})^\top \in \mathcal{D},$$

$$p = (p_{1,1}, \dots, p_{1,d}, \dots, p_{N,1}, \dots, p_{N,d})^\top \in \mathbb{R}^{dN},$$

where $q_i := (q_{i,1}, \dots, q_{i,d})^\top$ is the position vector of the i -th particle, and similarly for p . Let

$$\mathcal{E} := \mathcal{D} \times \mathbb{R}^{dN}.$$

Central objects in our study will be trajectories

$$(q_t, p_t)_{t \geq 0} \subset \mathcal{E},$$

which describe the time evolution of a physical system.

It is not clear *a priori* why we should choose momenta to describe the kinetic quality of the system, rather than velocities. However it is of no importance since we can change from one description to the other via the relation

$$v = M^{-1}p,$$

where $M \in \mathbb{R}^{dN \times dN}$ is a diagonal matrix recording the masses of each particle (d times per particle), and v is the velocity vector.

1.1.2 Dynamical description

In order to describe the evolution of the system's state, one must specify a dynamical law. This is done by giving a function $V : \mathcal{E} \rightarrow \mathbb{R}$ whose gradient in the i -th particle's coordinates

$$\nabla_{q_i} V := (\partial_{q_{i,d}}, \dots, \partial_{q_{i,d}})^\top$$

gives minus the force vector acting on the i -th particle. In our case we will always take the potential to be independent of the momentum, so that we can think of V as having domain \mathcal{D} . In the case where $\mathcal{D} = (L\mathbb{T})^{dN}$, it will be convenient to think of V as a function from \mathbb{R}^{dN} to \mathbb{R} which is C^1 and L -periodic in each direction. The function V is called the potential, and, as it encodes the dynamics of the system, it is of paramount importance. The time evolution of the system, then, is described by Newton's second law:

$$\frac{dp}{dt} = -\nabla V(q)$$

It will be convenient for our analysis to use of reformulation of Newton's equations, based on the Hamiltonian of a system.

Definition 2 (Hamiltonian). *The Hamiltonian of a classical system is its total energy, which is the sum of a kinetic energy term depending only on the momenta and a potential energy term depending only on the positions.*

$$(1.1) \quad H(q, p) = \frac{1}{2}p^\top M^{-1}p + V(q)$$

Using the Hamiltonian, we can rewrite the classical equations of motion as

$$(1.2) \quad \begin{cases} dq_t = M^{-1}p_t dt = \nabla_p H(q_t, p_t) dt \\ dp_t = -\nabla V(q_t) dt = -\nabla_q H(q_t, p_t) dt \end{cases},$$

The potential is the most important part of the microscopic description, and accordingly, the main problem in establishing a physical model of this kind is to determine potential functions which adequately capture the dynamic behavior of a given system. The choice of a classical description automatically implies a degree of approximation, since behavior arising from the laws of quantum mechanics, which may be relevant at a microscopic level, are described by Newton's law. Furthermore, if the aim is to simulate such systems numerically, computational constraints imply that some compromise has to be reached between theoretical accuracy and computational cost. If, for small systems, it may be possible to simulate all atomic interactions, for larger or more complex systems, it is often to use potential functions which are both cheap from a computational point of view and empirically shown to be accurate enough for the purpose of a simulation.

Our main numerical example will be the system given by the following potential, which is of this empirical form, and which is often used to describe the microscopic behavior of chemically inert fluids, such as Argon.

Example 1 (The Lennard-Jones fluid). We fix $L > 0$, $d = 3$, and N the number of particles. The Lennard-Jones fluid is the classical system given by the pair-interaction potential

$$(1.3) \quad V_{\text{LJ}}(q) = \sum_{1 \leq i < j \leq N} v(|q_i - q_j|),$$

where v is a radial function

$$v(r) = 4\varepsilon \left(\left(\frac{\sigma}{r}\right)^{12} - \left(\frac{\sigma}{r}\right)^6 \right).$$

The reference energy ε and length σ are shape parameters which respectively control the depth of the potential well of v and the equilibrium distance $2^{1/6}\sigma$. As seen on Figure 1.1, the potential combines two effects. At small interparticular distances, the dominant term is in r^{-12} , which translates into a strongly repulsive force between close pairs of particles, and makes individual particles essentially impenetrable. At long range, the dominant term is in $-r^6$, which translates into a weakly attractive force between distant particles. Contrary to the repulsive term, which is empirical, this scaling has a theoretical origin in the Van der Waals forces. From a computational standpoint, the fact that v is an even function of r allows one to compute the normalized force while sparing the expense of computing a square root, while the identity $r^{12} = (r^6)^2$ allows further economy. The shape parameters σ and ε must be chosen empirically to describe the behavior of a particular atomic species. For Argon, values of reference are: $\sigma =$, $\varepsilon =$.

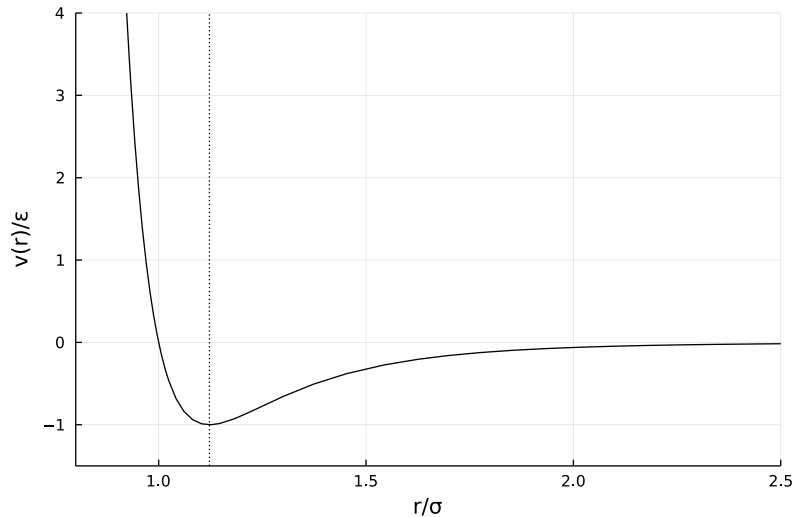


Figure 1.1: The pair potential v , with lengths and energy given in reduced units. The equilibrium interparticular distance is indicated by the vertical dotted line.

1.1.3 Reduced units

It is convenient, given an atomic system, to describe quantities therein within a system of units in which they are of order one. This has several advantages. Firstly, like any reasonable system of units, they make quantities easier and more intuitive to reason about. Secondly, from the computational point of view, numerical artifacts due to loss of precision at very large or very small scales and overflow errors can be avoided more often. Thirdly, they may help transfer knowledge about one system to another. For instance, in the Lennard-Jones system, expressing a

quantity in reduced units, and knowing the dependency of these units on the parameters (ε, σ, M) of the system, one can infer properties about a system with parameters $(\tilde{\varepsilon}, \tilde{\sigma}, \tilde{M})$ by applying the inverse transformation, thus effectively yielding equivalence of different systems under different conditions, and sparing the cost of running redundant simulations.

We describe a general procedure to construct a set of reduced units. Our choice, although not necessarily unique, is quite natural, especially when dealing with the Lennard-Jones system. Let us fix a reference mass m_* , a reference energy ε_* and a reference length σ_* . Then various reference quantities can be derived by natural conversions and dimensional analysis:

$$\begin{aligned} (\text{time}) \quad t_* &= \sqrt{\sigma_*^2 m_* \varepsilon_*^{-1}}, \\ (\text{temperature}) \quad T_* &= \varepsilon_* k_B^{-1}, \\ (\text{velocity}) \quad v_* &= \sigma_* t_*^{-1}, \\ (\text{volume}) \quad V_* &= \sigma_*^3, \\ (\text{area}) \quad A_* &= \sigma_*^2, \\ (\text{density}) \quad \rho_* &= V_*^{-1}, \\ (\text{force}) \quad F_* &= m_* \sigma_* t_*^{-2}, \\ (\text{pressure}) \quad P_* &= F_* A_*^{-1}, \end{aligned}$$

and one can of course go on. The point is that if X is a quantity, one can obtain its reduced value X_{red} by dividing X by the reference quantity X_* which is dimensionally compatible with X , and which can be derived as above. For instance, given a pressure P , we obtain

$$P_{\text{red}} = P \sigma_*^3 \varepsilon_*^{-1}.$$

Note this is an adimensional quantity. Note, also that, due to the definition of the reference temperature T_* relative to the reference energy ε_* , energy are now commensurate to temperatures. The Boltzmann factor, which is the conversion factor between units of temperature and units of energy simplifies when expressed in reduced units, a fact we can capture with the maxim $k_B* = 1$. This simplifies many formulae.

For a monoatomic Lennard-Jones system, a natural choice for m_* is the atomic mass of the considered species. We also take $\varepsilon_* = \varepsilon$ and $\sigma_* = \sigma$, (although the equilibrium length $\sigma = 2^{1/6}\sigma$ is another possible choice). In the case of Argon, we use the following values:

$$m_* = 6.634 \times 10^{-26} \text{ kg}, \quad \sigma_* = 3.405 \times 10^{-10} \text{ m}, \quad \varepsilon_* = 1.66 \times 10^{-21} \text{ J}.$$

Unless explicitly specified, all numerical results will be in this system of reduced units.

1.2 Statistical ensembles

The microscopic description is interesting from a theoretical standpoint, but it fails to be relevant when attempting to describe the behavior of atomic systems with a macroscopic number of particles, of the order of Avogadro's number (6.02×10^{23}). Besides the technical impossibility of measuring to a high accuracy the configuration of such systems, and that of recording the information required to track it (coincidentally, the total amount of digitally stored information on Earth is estimated to be 10^{23} bytes as of 2022), it is also the case that knowledge of a system at this level of detail is unnecessary to describe the quantities which are relevant to our macroscopic experience. In the instance of a gas at thermal equilibrium, examples of relevant quantities are total energy, pressure, temperature, density, which, while of course resulting from the internal state of the system, are independent of the minutiae of individual atomic motions: loosely speaking, one may describe the macroscopic state of a system by only a handful of macroscopic variables, loosing track of the myriad of microscopic degrees of freedom. An important point is that for a given macroscopic state, there are many microscopic configurations which are

compatible with our observations. This motivates defining the macroscopic state of a system as a probability distribution over phase space, which we may interpret as assigning to each microscopic configuration a likelihood that this configuration underlies the macroscopic state.

This does not tell one how to choose the distribution over microscopic states. However, it seems reasonable to assign positive probabilities to states compatible with the macroscopic constraints, and in such a way as to make the weakest possible assumptions on this microscopic state, or in other words contain the least amount of information about the system, given the macroscopic constraints. The mathematical translation of this idea is given by the principle of maximal entropy. Given a class of probability distributions compatible with the macroscopic constraints, define the macroscopic state as the one which maximizes the entropy, which is defined for a probability distribution ρ by

$$(1.4) \quad \mathfrak{S}(\rho) = - \int_{\mathcal{E}} \rho(x) \ln(\rho(x)) dx.$$

The specification of a probability distribution over states is called a thermodynamic ensemble. We will be considering the following two examples.

1.2.1 Microcanonical ensemble

The microcanonical ensemble is the suitable model for an isolated system in thermodynamic equilibrium, evolving under Hamiltonian dynamics. The number of particles N , the volume $V = L^3$, and the energy E is fixed. We will alternatively refer to the microcanonical ensemble as the NVE ensemble. Because the constant energy condition constrains the compatible microstates to level sets of H , which in general will be negligible subsets of \mathcal{E} , some care must be taken in defining the microcanonical measure, since one cannot express the macroscopic constraints by a family of probability densities. However, under suitable assumptions on V , one can define the microcanonical measure as a weak limit of uniform distributions over level ‘‘shells’’ of H :

$$\int_{\mathcal{E}} \varphi d\mu_{\text{NVE}} := \lim_{\varepsilon \rightarrow 0} \frac{1}{|S(E, \varepsilon)|} \int_{S(E, \varepsilon)} \varphi(q, p) dq dp,$$

where

$$S(E, \varepsilon) = \{(q, p) \in \mathcal{E} \mid H(q, p) \in [E - \varepsilon, E + \varepsilon]\}.$$

This is consistent with the fact that, for a set A with finite Lebesgue measure, the probability distribution on A which maximizes the entropy is the uniform distribution on A . It is possible, using the coarea formula, to derive a precise expression for this limit, namely,

$$(1.5) \quad \mu_{\text{NVE}}(dq, dp) = \frac{\sigma_{\mathbb{E}}(dq, dp)}{|\nabla H(q, p)|}$$

1.2.2 Canonical ensemble

Isolated systems in thermal equilibrium are not typically those that we encounter in experiments. Instead, it is more common to observe systems which are in thermal equilibrium with respect to their environment, an ambient *heat bath* at a fixed temperature. The total energy of such systems is not fixed: small fluctuations can occur as energy is exchanged back and forth between the heat bath and the system. However, the average energy \bar{E} is fixed. This is the macroscopic constraint that defines the canonical ensemble. For a fixed N, V, \bar{E} , define the density of the the canonical measure as the maximizer:

$$\operatorname{argmax}_{\rho \in \mathcal{A}} \mathfrak{S}(\rho)$$

where \mathcal{A} is the set of admissible densities

$$\mathcal{A} = \left\{ \rho : \mathcal{E} \mapsto \mathbb{R}_+ \mid \int_{\mathcal{E}} \rho = 1, \int_{\mathcal{E}} H(q, p) \rho(q, p) dq dp = E \right\}.$$

Solving the Euler-Lagrange equation associated with this constrained optimization problem yields that the only admissible solution can be written under the form:

$$\rho^*(q, p) = \frac{1}{Z} e^{-\beta H(q, p)}.$$

Furthermore, one can show that ρ^* is indeed the unique maximizer. Here, $-\beta$ and $1 + \ln Z$ are the critical Lagrange multipliers associated respectively with the energy constraint and the normalization constraint. Thus

$$Z = \int_{\mathcal{E}} e^{-\beta H(q, p)} dq dp$$

is a normalization constant called the partition function, and β is a tuning parameter related to the value of \bar{E} . The physical interpretation of β is that of an inverse temperature,

$$\beta = \frac{1}{k_B T},$$

where $k_B = 1.38 \times 10^{-23} \text{ J} \cdot \text{K}^{-1}$ is Boltzmann's constant. For obvious reasons, we prefer to refer to the canonical ensemble as the NVT ensemble (rather than the NVE)

One could of course go further and remark that when observing a fixed volume of unconfined gas in thermal equilibrium, the total number of particles N is not fixed. Instead, this fluctuates as particles are constantly exchanged with an ambient particle reservoir. Instead, the average number of particles \bar{N} is fixed. The resulting ensemble is called the grand canonical or μ VT ensemble. This, and many other constructions are possible, but we will restrict our attention to the NVE and NVT cases.

Remark 1. We can make an observation on μ using the fact that the Hamiltonian 1.1 is separable: it is the sum of a kinetic term involving p and a configurational term involving q . Thus we can write

$$e^{-\beta H(q, p)} = e^{-\frac{\beta}{2} p^\top M^{-1} p} e^{-\beta V(q)},$$

which implies that the canonical measure μ is of tensor form:

$$\mu = \kappa \otimes \nu,$$

where κ is a probability measure on \mathbb{R}^{dN} has a density proportional to $e^{-\frac{\beta}{2} p^\top M^{-1} p}$ and ν has a density proportional to $e^{-\beta V(q)}$ on \mathcal{D} . Recognizing a multivariate Gaussian density, we can further write, abusing the notations κ and ν to denote both the laws and their densities,

$$(1.6) \quad \kappa(p) = \det\left(\frac{\beta M}{2\pi}\right)^{\frac{1}{2}} e^{-\frac{\beta}{2} p^\top M^{-1} p}$$

$$(1.7) \quad \nu(p) = \frac{1}{Z_\nu} e^{-\beta V(q)},$$

with

$$Z_\nu = Z \det\left(\frac{\beta M}{2\pi}\right)^{\frac{1}{2}}.$$

This implies in particular that the marginal distribution in p of the canonical measure can be sampled easily, using standard algorithms for generating i.i.d. Gaussian variables, such as the Box-Muller method.

The difficult part is sampling ν . Why we should even care to do so is the object of the following paragraph.

1.2.3 From microscopic dynamics to macroscopic observables

The main interest in describing the macroscopic state of a system as a probability distribution over its microscopic configurations is that one can then express constant macroscopic quantities as averages of fluctuating microscopic observables with respect to the ensemble measure. In our context, an observable is simply a function defined over phase-space. Given a macroscopic system defined by an equilibrium ensemble μ and an observable φ , we are interested in computing its average value over the ensemble,

$$(1.8) \quad \mathbb{E}_\mu[\varphi] := \int_{\mathcal{E}} \varphi(q, p) \mu(dq, dp).$$

Two problems arise. One is, for a given macroscopic quantity of interest, how to define the microscopic observable φ which corresponds to this quantity. The second, once we have properly defined φ , is how to compute averages (??).

1.2.4 Examples of instantaneous observables

Let us give some examples of observables which will be of interest to us. Obvious examples include the kinetic energy,

$$E_\kappa(q, p) = \frac{1}{2} p^\top M^{-1} p,$$

the potential energy

$$E_p(q, p) = V(q),$$

and the Hamiltonian H . We will generally be considering real-valued observables, although vector-valued observables such as the velocity $v = M^{-1}p$ may be of interest. We will give two additional examples. The kinetic temperature is defined by the following expression:

$$T_\kappa(q, p) = \frac{2}{k_B d N} E_\kappa(q, p).$$

It is, up to a conversion factor of Boltzmann's constant, twice the kinetic energy per degree of freedom. In the canonical ensemble, it is easily shown that $\mathbb{E}_\mu[T_\kappa] = T$, justifying the terminology. (reference also equipartition theorem)

We will also be considering the instantaneous pressure, which is given, for a pair interaction potential of the form (1.3) and a periodic domain \mathcal{D}

$$P(q, p) = \frac{1}{|\mathcal{D}|} \left(N k_B T_\kappa - \frac{1}{d} \sum_{i=1}^N q_i^\top \nabla_{q_i} V(q) \right).$$

Neglecting the right-hand side gives the famous ideal gas law, $PV = Nk_B T$, which is a good approximation at low densities. The right hand side, otherwise known as the virial, appears to be problematic since the q_i are not periodic functions of q , which would suggest P is not a well-defined observable on \mathcal{D} . However, using the particular form of the potential, which is a function of the displacements $|q_i - q_j|$, and symmetry arising from Newton's third law, we can arrive at the following expression:

$$P(q, p) = \frac{1}{d|\mathcal{D}|} \left(\sum_{i=1}^N \frac{|p_i|}{m_i} - \sum_{i \neq j} |q_i - q_j| v'(|q_i - q_j|) \right),$$

which is indeed a periodic function of q . In the NVT ensemble, the average of the kinetic part of the pressure is a known parameter, so we may replace it by its value, considering the observable:

$$\frac{N}{\beta |\mathcal{D}|} - \frac{1}{d|\mathcal{D}|} \sum_{i=1}^N q_i^\top \nabla_{q_i} V(q).$$

1.2.5 Ergodic averages

This second problem is one of sampling a probability measure in many dimensions, which is a difficult problem in general. Our broad strategy, which will remain the same in the NVE and NVT case, is the following. We define a process $(q_t, p_t)_{t \geq 0}$ on \mathcal{E} , either deterministic or stochastic, which is invariant for the target measure μ , in the following sense:

$$(1.9) \quad \forall t \geq 0, \varphi \in B^\infty(\mathcal{E}), \int_{\mathcal{E}} \mathbb{E}^{(q,p)} [\varphi(q_t, p_t)] \mu(dq, dp) = \int_{\mathcal{E}} \varphi(q, p) \mu(dq, dp),$$

where the superscript in the expectation denotes that the process has value (q, p) at $t = 0$, and the expectation is over values of (q_t, p_t) . In other words, this is a process which, given that its initial condition is distributed according to μ , remains distributed according to μ at any later time. It is then natural to consider average values of φ over the trajectories:

$$(1.10) \quad \frac{1}{T} \int_0^T \varphi(q_t, p_t) dt,$$

which we may hope will converge to the target value. The convergence of ergodic averages to the ensemble average can be shown not to hold in generality, and is something which must be proven on a case by case basis, though general criteria can be derived. If the underlying dynamic is stochastic, then the variance of the random variables (1.10) becomes an issue, which one must keep in check by ensuring that time averages are taken over long enough trajectories. Furthermore, since the true invariant dynamics is in general in continuous time, one must devise discrete in time approximations to the true trajectories. However, empirical practice shows that ergodic averages obtained from computer simulations, even for a modest number of atoms, agrees very well with experimental data for certain types of systems, and even in the absence of theoretical guarantees.

Chapter 2

Sampling equilibrium ensembles

2.1 Properties of Hamiltonian dynamics

2.2 Microcanonical averages

Our aim in this section will be to describe methods to sample microcanonical averages. We will always consider microcanonical averages as ergodic averages under Hamiltonian trajectories. To justify this approach, we should make sure that the microcanonical measure is invariant under the Hamiltonian dynamics. Indeed, this is the case:

The Hamiltonian dynamics (1.2) rewrites in matrix form, writing $X_t = (q_t, p_t)$:

$$(2.1) \quad dX_t = J \nabla H(X_t) dt,$$

where J is the symplectic matrix

$$J = \begin{pmatrix} 0_{dN} & \text{Id}_{dN} \\ -\text{Id}_{dN} & 0_{dN} \end{pmatrix}$$

This will be useful to investigate properties of the Hamiltonian dynamics. Applying the chain rule to any smooth function $\varphi : \mathcal{S} \mapsto \mathbb{R}$, we obtain

$$d\varphi(X_t) = dX_t^\top \nabla \varphi(X_t) = (J \nabla H(X_t))^\top \nabla \varphi(X_t) dt = (\nabla_p H \cdot \nabla_q - \nabla_q H \cdot \nabla_p) \varphi(X_t) dt$$

This motivates the following.

Definition 3 (Generator of the Hamiltonian dynamics). *We define the generator associated with the Hamiltonian dynamics to be the operator \mathcal{L}_H defined on smooth functions by*

$$(2.2) \quad \mathcal{L}_{\text{ham}} \varphi = (\nabla_p H \cdot \nabla_q - \nabla_q H \cdot \nabla_p) \varphi = (J \nabla H)^\top \nabla \varphi$$

We can split the generator as the sum of two elementary operators,

$$\mathcal{L}_{\text{ham}} = A + B,$$

with

$$(2.3) \quad A = (M^{-1}p) \cdot \nabla_q \quad B = -\nabla V(q) \cdot \nabla_p.$$

The generator allows us to quantify the rate of change of an observable φ under the evolution of the system. If we define, for $t \geq 0$, the evolution operators

$$P_t \varphi(q_0, p_0) = \varphi(\Phi_t(q_0, p_0)),$$

where Φ is the flow associated with the Hamiltonian dynamics, that is the collection of maps $(\Phi_t)_{t \geq 0}$, defined by $\Phi_t(q_0, p_0) = (q_t, p_t)$, the solution to (1.2) with initial conditions (q_0, p_0) , then we have formally:

$$\frac{\partial}{\partial t} P_t \varphi(q, p) = \partial_t \varphi(q_t, p_t) = \mathcal{L}_{\text{ham}} \varphi(q_t, p_t) = \mathcal{L}_{\text{ham}} P_t \varphi(q, p) = P_t \mathcal{L}_{\text{ham}} \varphi(q, p).$$

Applying \mathcal{L}_{ham} to H immediately gives the following result.

Proposition 1 (Energy conservation).

$$(2.4) \quad dH(X_t) = 0$$

This relation expresses the fact that the Hamiltonian is invariant under the flow of (1.2). This, in turn, is the mathematical translation of the physical principle of conservation of energy. Using the fact that the Hamiltonian flow field is divergence-free,

$$(2.5) \quad \operatorname{div}(J \nabla H) = \operatorname{div}_q(\nabla_p H) - \operatorname{div}_p(\nabla_q H) = 0,$$

one can show the following property, famously known as Liouville's theorem.

Proposition 2 (Conservation of volume). *For any measurable set $D \subset \mathcal{E}$, we have*

$$(2.6) \quad |\Phi_t(D)| = |D|.$$

Definition 4 (Symplecticity). *A mapping φ from \mathbb{R}^{2d} to itself is said to be symplectic on some open set $U \subset \mathbb{R}^{2d}$ if it is C^1 and if, for all $(q, p) \in U$,*

$$\nabla \varphi^\top J \nabla \varphi = J,$$

where $\nabla \varphi$ is the Jacobian matrix of φ (C.1).

Proposition 3. *For any $t \in \mathbb{R}$, the Hamiltonian flow Φ_t is symplectic.*

Consider the momentum-reversing map

$$(2.7) \quad \mathcal{R}(q, p) = (q, -p)$$

We then have the following time symmetry property.

Proposition 4 (Time symmetry).

$$(2.8) \quad \Phi_t \circ \mathcal{R} \circ \Phi_t = \text{Id}$$

Remark 2. *The property (2.4) is only due to the form of J , and not to the specific expression for H . Thus any H , we may consider any dynamics of the form (2.1), to devise a dynamical system whose orbits are restricted to the level set $H^{-1}\{H(q_0, p_0)\}$.*

Conversely, given a differential dynamical system, if through a change of coordinates one is able to write the system under this form, one has found a conservation law.

An important remark is that if one considers each part of (2.3) as a generator in itself, the corresponding dynamics is analytically solvable.

Remark 3. *Consider the two dynamics defined by*

$$(2.9) \quad \begin{cases} dq_t^A = M^{-1} p_t^A dt, & dp_t^A = 0, \\ dq_t^B = 0, & dp_t^B = -\nabla V(q_t^B) dt. \end{cases}$$

These are easily solved, namely

$$(2.10) \quad \begin{cases} (q_t^A, p_t^A) = (q_0^A + tp_0^A, p_0^A), \\ (q_t^B, p_t^B) = (q_0^B, p_0^B - tV(q_0^B)). \end{cases}$$

Moreover, these evolutions are of Hamiltonian form, with Hamiltonians corresponding respectively to the kinetic part and the configurational part only, and have corresponding generators A and B . We denote by $(\Phi_t^A)_{t \geq 0}$ and $(\Phi_t^B)_{t \geq 0}$ their respective flows. This splitting property will prove useful in constructing numerical schemes for both Hamiltonian and stochastic dynamics.

2.2.1 Numerical schemes for Hamiltonian dynamics

It is impossible, except for a very restricted class of systems, which do not occur in practical settings anyhow, to analytically integrate Hamilton's equation (1.2). For this reason, one must revert to numerical schemes, which we may interpret as discrete approximations of the Hamiltonian flow. More precisely, for a fixed timestep Δt , if we possess an approximation of the flow

$$\tilde{\Phi}_{\Delta t} \approx \Phi_{\Delta t},$$

we will deduce approximations of the evolution

$$(2.11) \quad (q^n, p^n) := \tilde{\Phi}_{\Delta t}^n(q_0, p_0) \approx (q_{n\Delta t}, p_{n\Delta t}),$$

which can then be used as sample points for the computation of empirical averages, discrete counterparts to the ergodic averages (1.10),

$$(2.12) \quad \frac{1}{n} \sum_{k=0}^n \varphi(q^n, p^n).$$

In most common applications, the aim is to approximate the exact solution of an evolution equation as precisely as possible over a given time domain. In the case of molecular dynamics, however, the time domain is usually very large, because simulating long trajectories is a requirement to ensure that a representative portion of phase space is explored. As a consequence, it is in practice impossible to obtain precise solutions over a long time, because of the evolution's sensitivity to the initial conditions. Furthermore, one does not even care about the exact evolution, since the dynamics are merely used as a sampling device. Instead, one key requirement is that the dynamics stay on or close to the constant Hamiltonian manifold associated with the initial conditions. It can be shown through eigenanalysis that for simple linear systems, this requirement is not satisfied by standard ODE numerical methods such as the explicit and implicit Euler schemes, or the RK4 method, for which the energy may explode or implode geometrically. This has the practical effect that for reasonably sized atomic systems, numerical instabilities render the simulations nonsensical after only a few time steps, a far cry from what is needed to obtain good estimates. One must then devise dedicated numerical methods, guided by the aim to preserve qualitative properties of the Hamiltonian evolution. It turns out that splitting schemes, based on operator splitting approximations of the Hamiltonian evolution operator over one timestep, preserve crucial qualitative properties of the Hamiltonian evolution. Let us fix a timestep $\Delta t > 0$. Numerical schemes aim to approximate the flow $\Phi_{\Delta t}$. Splitting schemes rely on the splitting property (2.10) to construct computable approximations

$$\Phi_{\Delta t} \approx \Phi_{\Delta t_k}^{G_k} \circ \dots \circ \Phi_{\Delta t_1}^{G_1},$$

where $G_i \in \{A, B\}$ for all i . We will be considering three schemes, the simplest of which are the symplectic Euler schemes.

The symplectic Euler schemes are defined by the following update equations.

$$(2.13) \quad \begin{cases} p^{n+1} = p^n - \nabla V(q^n)\Delta t \\ q^{n+1} = q^n + M^{-1}p^{n+1}\Delta t \end{cases}$$

$$(2.14) \quad \begin{cases} q^{n+1} = q^n + M^{-1}p^n\Delta t \\ p^{n+1} = p^n - \nabla V(q^{n+1})\Delta t \end{cases}$$

These correspond respectively to the splitting approximations

$$\Phi_{\Delta t} \approx \Phi_{\Delta t}^A \circ \Phi_{\Delta t}^B := \Phi_{\Delta t}^{BA}$$

and

$$\Phi_{\Delta t} \approx \Phi_{\Delta t}^B \circ \Phi_{\Delta t}^A := \Phi_{\Delta t}^{AB}.$$

The velocity Verlet scheme is based on the splitting

$$\Phi_{\Delta t} \approx \Phi_{\Delta t/2}^B \circ \Phi_{\Delta t}^A \circ \Phi_{\Delta t/2}^B := \Phi_{\Delta t}^{BAB}.$$

Its update equation is given by

$$(2.15) \quad \begin{cases} p^{n+\frac{1}{2}} = p^n - \frac{\Delta t}{2} \nabla V(q^n) \\ q^{n+1} = q^n + \Delta t M^{-1} p^{n+\frac{1}{2}} \\ p^{n+1} = p^{n+\frac{1}{2}} - \frac{\Delta t}{2} \nabla V(q^{n+1}). \end{cases}$$

2.2.2 Properties of symplectic schemes

The main interest of these schemes is that, as hinted at above, they preserve some qualitative properties of Hamiltonian dynamics, which are essential if the aim is to compute ergodic averages. One, which relies on the simple observation that the composition of two symplectic mappings is symplectic, is the following proposition.

Proposition 5. *The mappings $\Phi_{\Delta t}^{AB}$, $\Phi_{\Delta t}^{BA}$ and $\Phi_{\Delta t}^{BAB}$ are symplectic, like any mapping obtained by composition of the Hamiltonian flows $\Phi_{\Delta t}^A$ and $\Phi_{\Delta t}^B$.*

One may ideally wish to guarantee that the Hamiltonian is preserved under the discrete evolution induced by these schemes. This, it turns out, is too high a hope. It happens, however, that, for each of these schemes, an approximate Hamiltonian is (almost) exactly conserved, which we can interpret to mean that the discrete dynamics (2.11) are (almost) exact sample points for a modified dynamics, corresponding to the modified Hamiltonian. The order of this modification in the timestep Δt then allows one to deduce the order of conservation of the original Hamiltonian. The proofs of this type of results fall under the umbrella of backward numerical analysis. For more information, refer to [3]. A precise statement is the following.

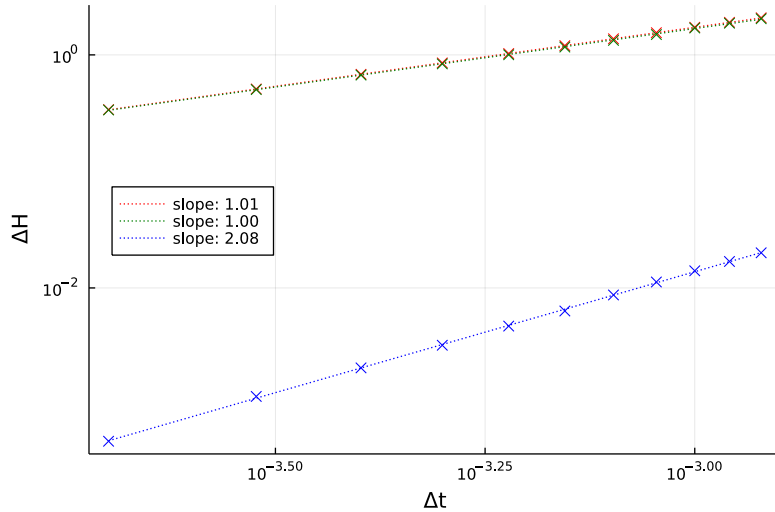


Figure 2.1: Effect of the time step on absolute variation of the Hamiltonian for the symplectic Euler (red and green) and the Verlet (blue) schemes. As expected, total variation scales as Δt for symplectic Euler, and as Δt^2 for Verlet.

2.2.3 Shortcomings of the Hamiltonian approach

2.3 Canonical averages

2.3.1 Langevin dynamics

We consider a special case of the inertial Langevin dynamics, defined by the following stochastic differential equation (SDE), where γ, β are fixed positive constants.

$$(2.16) \quad \begin{cases} dq_t = M^{-1} p_t dt, \\ dp_t = -\nabla V(q_t) dt - \gamma M^{-1} p_t dt + \sqrt{\frac{2\gamma}{\beta}} dW_t, \end{cases}$$

where $(W_t)_{t \geq 0}$ is a standard dN -dimensional Brownian motion. This process is a combination of a Hamiltonian evolution with an additional action on the momenta which, if isolated, defines a dN -dimensional Ornstein-Uhlenbeck process.

This additional term be interpreted physically as the combination of two effects: a dissipation term

$$-\gamma M^{-1} p_t dt,$$

which can be understood as the effect of a viscous friction force on the particles, and a fluctuation term,

$$\sqrt{\frac{2\gamma}{\beta}} dW_t,$$

which corresponds to the input of kinetic energy into the system as thermal agitation induced by a surrounding heat bath at temperature $1/(k_B \beta)$.

However, the physical meaning can be forgotten thanks to the fact that, *in fine*, we only require that the canonical measure be invariant under this dynamic: as we shall shortly see, this is indeed the case.

Remark 4. *There are several ways to generalize this process: one is to consider more general, possibly non-separable, Hamiltonians, as in Remark 2, rather than the classical Hamiltonian used above. The other is to allow the fluctuation-dissipation term to be parametrized by coefficients γ and σ depending on the state variable, and which obey a relation ensuring the invariance of μ . Hence in full generality, we could consider the following Langevin dynamic:*

$$(2.17) \quad \begin{cases} dq_t = \nabla_p H(q_t, p_t) dt, \\ dp_t = -\nabla_q H(q_t, p_t) dt - \gamma(q_t, p_t) \nabla_p H(q_t, p_t) dt + \sigma(q_t, p_t) dW_t. \end{cases}$$

The generator of the Langevin dynamics is the operator

$$(2.18) \quad \mathcal{L}_\gamma = M^{-1} p \cdot \nabla_q - \nabla V(q) \cdot \nabla_p - \gamma M^{-1} p \cdot \nabla_p + \frac{\gamma}{\beta} \Delta_p,$$

which splits into three elementary generators, namely

$$\mathcal{L}_\gamma = A + B + \gamma C = \mathcal{L}_{\text{ham}} + \gamma C,$$

with

$$(2.19) \quad C = -M^{-1} p \cdot \nabla_p + \frac{1}{\beta} \Delta_p.$$

These generators individually give rise to dynamics which we can express explicitly, defined by the following evolution operators:

$$(2.20) \quad \begin{cases} e^{tA}\varphi(q, p) = \varphi(q + tM^{-1}p, p), \\ e^{tB}\varphi(q, p) = \varphi(q, p - t\nabla V(q)), \\ e^{t\gamma C}\varphi(q, p) = \mathbb{E} \left[\varphi \left(q, e^{-\gamma M^{-1}t}p + \sqrt{\frac{M}{\beta}(1 - e^{-2\gamma M^{-1}t})}G \right) \right], \end{cases}$$

where G is a standard dN -dimensional Gaussian. The third equality translates an equality in law between an Itô integral and a Gaussian random variable, and follows by applying Itô's formula to the rescaled process

$$e^{\gamma M^{-1}t}X_t,$$

where X_t is the Ornstein-Uhlenbeck process:

$$(2.21) \quad dX_t = -\gamma M^{-1}X_t dt + \sqrt{\frac{2\gamma}{\beta}}dW_t.$$

The dynamics associated with the A and B part are deterministic Hamiltonian dynamics already identified in (2.10).

2.3.2 Properties of the Langevin dynamics

Invariance of the canonical measure

Using the generator, one can easily express the evolution of a probability distribution under the Langevin dynamics. We assume that the solution $(q_t, p_t)_{t \geq 0}$ to (2.16) has a distribution with a smooth density ρ_0 over \mathcal{E} at time $t = 0$, and denote ρ_t the probability density of (q_t, p_t) . For any test observable φ , we have

$$\int_{\mathcal{E}} \varphi(q, p) \rho_t(q, p) dq dp = \int_{\mathcal{E}} \mathbb{E}^{(q, p)} [\varphi(q_t, p_t)] \rho_0(q, p) dq dp = \int_{\mathcal{E}} e^{t\mathcal{L}_\gamma} \varphi(q, p) \rho_0(q, p) dq dp,$$

where the superscript is as in (1.9). Thus,

$$\frac{\partial}{\partial t} \int_{\mathcal{E}} \varphi(q, p) \rho_t(q, p) dq dp = \int_{\mathcal{E}} e^{t\mathcal{L}_\gamma} \mathcal{L}_\gamma \varphi(q, p) \rho_0(q, p) dq dp = \int_{\mathcal{E}} \mathcal{L}_\gamma \varphi(q, p) \rho_t(q, p) dq dp$$

If we define $\mathcal{L}_\gamma^\dagger$ as the adjoint of \mathcal{L}_γ on the flat space $L^2(\mathcal{E})$, that is,

$$(2.22) \quad \int_{\mathcal{E}} \mathcal{L}_\gamma \varphi \psi = \int_{\mathcal{E}} \varphi \mathcal{L}_\gamma^\dagger \psi \quad \text{for all test functions } \phi, \psi,$$

we have the Fokker-Planck equation,

$$(2.23) \quad \frac{\partial}{\partial t} \int_{\mathcal{E}} \varphi(q, p) \rho_t(q, p) dq dp = \int_{\mathcal{E}} \varphi(q, p) \mathcal{L}_\gamma^\dagger \rho_t(q, p) dq dp,$$

which rewrites formally as

$$(2.24) \quad \frac{\partial}{\partial t} \rho_t = \mathcal{L}_\gamma^\dagger \rho_t.$$

Using this equation, we can easily show that the canonical distribution is invariant under this dynamics, which is equivalent to the condition

$$\mathcal{L}_\gamma^\dagger \mu = 0.$$

In fact, it is useful to reformulate this condition in the weighted space $L^2(\mu)$. Indeed, the stationary Fokker-Planck equation rewrites

$$\int_{\mathcal{E}} \mathcal{L}_\gamma \varphi d\mu = 0 \quad \forall \varphi,$$

or

$$\int_{\mathcal{E}} (\mathcal{L}_\gamma^* \mathbb{1}_{\mathcal{E}}) \varphi d\mu \quad \forall \varphi,$$

where \mathcal{L}_γ^* is the adjoint of \mathcal{L}_γ in $L^2(\mu)$ under the scalar product

$$\langle \varphi, \psi \rangle_\mu := \int_{\mathcal{E}} \varphi \psi d\mu.$$

This, in turn, follows easily from the following lemma.

Lemma 1. *The $L^2(\mu)$ adjoints of the elementary differential operators are given by the formulae*

$$(2.25) \quad \begin{cases} \partial_{q_i}^* = -\partial_{q_i} + \beta \partial_{q_i} V, \\ \partial_{p_i}^* = -\partial_{p_i} + \beta (M^{-1} p)_i. \end{cases}$$

These are easily found by integration by parts. In particular, we find that

$$\partial_{q_i} \partial_{p_i}^* - \partial_{p_i} \partial_{q_i}^* = \beta ((M^{-1} p)_i \partial_{q_i} - \partial_{q_i} V \partial_{p_i}),$$

whence, by summing over i , we get

$$(2.26) \quad \mathcal{L}_{\text{ham}} = \frac{1}{\beta} (\nabla_q \cdot \nabla_p^* - \nabla_p \cdot \nabla_q^*),$$

which is an antisymmetric operator. Similarly,

$$\partial_{p_i} \partial_{p_i}^* = \beta (M^{-1} p)_i \partial_{p_i} - \partial_{p_i}^2,$$

hence

$$(2.27) \quad C = -\frac{1}{\beta} \nabla_p \cdot \nabla_p^*,$$

which is a symmetric operator. In summary, we have that

$$(2.28) \quad \mathcal{L}_\gamma^* = -\mathcal{L}_{\text{ham}} + \gamma C = -(A + B) + \gamma C.$$

It follows immediately that $\mathcal{L}_\gamma^* \mathbb{1}_{\mathcal{E}} = 0$. Notice that since $\mathcal{L}_{\text{ham}}^* \mathbb{1}_{\mathcal{E}} = 0$, the canonical measure is also invariant under the Hamiltonian dynamics. However, because of the energy conservation property (2.4), ergodic averages cannot in general converge to their averages under μ .

Convergence to equilibrium

2.3.3 Overdamped limit of Langevin dynamics

As already pointed out, the fact that the kinetic marginal of μ is a Gaussian distribution makes sampling canonical momenta trivial. Instead, the main problem is sampling from ν . It follows directly from the invariance of μ under trajectories of the Langevin dynamics that ν is invariant under the configurational trajectories of the Langevin dynamics. It would be convenient, however, to have at our disposal a dynamics on \mathcal{D} which has ν as an invariant measure. It turns out this is possible, by observing that the invariance of μ is independent of the parameter γ , and taking the limit $\gamma \rightarrow \infty$. This requires some care. Notice the SDE on the momenta in (2.16) rewrites

$$dp_t = -\nabla V(q_t)dt - \gamma dq_t + \sqrt{\frac{2\gamma}{\beta}} dW_t,$$

thus integrating gives

$$q_t - q_0 = \frac{p_0 - p_t}{\gamma} - \frac{1}{\gamma} \int_0^t \nabla V(q_s) ds + \sqrt{\frac{2}{\gamma\beta}} W_t.$$

The scaling invariance of the Brownian motion $(\sqrt{\alpha}W_{t/\alpha^2})_{t \geq 0} \sim (W_t)_{t \geq 0}$ suggests considering the timescale $\gamma\beta t$, thus

$$q_{\gamma\beta t} - q_0 = \frac{p_0 - p_{\gamma\beta t}}{\gamma} - \frac{1}{\gamma} \int_0^{\gamma\beta t} \nabla V(q_s) ds + \sqrt{2} \widetilde{W}_t,$$

where \widetilde{W} is again a Brownian motion. Using the change of variables $s = \gamma\beta u$ in the integral term yields

$$(2.29) \quad q_{\gamma\beta t} - q_0 = \frac{p_0 - p_{\gamma\beta t}}{\gamma} - \beta \int_0^t \nabla V(q_{\gamma\beta u}) du + \sqrt{2} \widetilde{W}_t,$$

At this point, we formally take $\gamma \rightarrow \infty$, which suggests the following SDE for the rescaled in time process,

$$(2.30) \quad dq_t = -\beta \nabla V(q_t) dt + \sqrt{2} dW_t.$$

This equation defines the overdamped Langevin, or Brownian, dynamics. To justify the limit in a rigorous manner, one would hope to show that the rescaled process (2.29) converges in law to a weak solution of the SDE (2.30), in some functional space. However, this is technical overkill, since, we only need to consider dynamics as sampling devices. In fact, the physical interpretation of this equation is not even clear in terms of the dimensions of the quantities at play. We can just as well take equation (2.30) as given, and be satisfied by the following fact.

Proposition 6. *The configurational Gibbs measure ν is invariant under the dynamics (2.30).*

This follows along the same lines as for the Langevin dynamics. The generator (now acting on observables defined on \mathcal{D}) is the operator

$$(2.31) \quad \mathcal{L}\varphi = -\beta \nabla V \cdot \nabla \varphi + \Delta \varphi.$$

Again, we consider the weighted space $L^2(\nu)$. Adjoints of elementary differential operators are still given by the first line of (2.25), and it is then easily seen that

$$(2.32) \quad \mathcal{L} = -\nabla^* \cdot \nabla$$

is a symmetric operator. Again we have $\mathcal{L}^* \mathbb{1}_{\mathcal{D}} = 0$, so ν satisfies the stationary Fokker-Planck equation under this dynamics.

Remark 5. *Instead of rescaling time by $\beta\gamma$, we could have rescaled by γ , which would yield the dynamics*

$$(2.33) \quad dq_t = -\nabla V(q_t) dt + \sqrt{\frac{2}{\gamma}} dW_t.$$

Which formulation to choose is a matter of preference, since both yield a dynamics invariant under ν , as seen from the identity (where we still write \mathcal{L} for the generator)

$$\mathcal{L} = -\frac{1}{\beta} \nabla^* \cdot \nabla.$$

As for the Langevin dynamics, it is possible to show tha

2.3.4 Splitting schemes for the Langevin dynamics

Just as in the Hamiltonian case, we can define schemes for the Langevin dynamics based on approximating the evolution operator over one timestep by splitting the generator \mathcal{L}_γ , and combining the corresponding evolution operators (2.20) in a sequence. We refer to such a splitting approximation by the sequence in which the individual propagators are composed. It is useful at this point to introduce the stochastic flow map associated with the Ornstein-Uhlenbeck dynamics.

$$(2.34) \quad \Phi_t^C(q, p, \xi) = \left(q, e^{-\gamma M^{-1}t} p + \sqrt{\frac{M}{\beta}(1 - e^{-2\gamma M^{-1}t})} \xi \right),$$

where $\xi \in \mathbb{R}^{dN}$, the point being $\mathbb{E}[\varphi(\Phi_t^C(q, p, G))] = e^{t\gamma C}\varphi(q, p)$ when G is standard Gaussian. Given an ordering of operators,

$$(2.35) \quad (R_1, \dots, R_k) \in \{A, B, \gamma C\}^k,$$

we can consider the mapping, which we note, by a slight abuse, as

$$(2.36) \quad \Phi^{R_1, \dots, R_k} := \Phi_{\Delta t/n_{R_k}}^{R_k} \circ \dots \circ \Phi_{\Delta t/n_{R_1}}^{R_1},$$

where

$$n_R := \#\{1 \leq j \leq n | R_j = R\}$$

for $R \in \{A, B, \gamma C\}$, and which we define to be the mapping which takes a point in phase space and $n_{\gamma C}$ vectors in $\mathbb{R}^{dN}(\xi_1, \dots, \xi_{n_{\gamma C}})$, yielding a point in phase space by successively applying the flow, and, if need be, stochastic flow, mappings corresponding to the reverse ordering of (2.35). Applying this mapping with a vector of independent standard Gaussians yields a stochastic mapping, which defines the update rule for the splitting scheme associated with the ordering (2.35). An important property which follows from writing the update rule using the mapping (2.36) is that numerical trajectories formed by iterating this update rule with independent vectors of standard Gaussians form a Markov chain. The hope is that the invariant measure corresponding to this Markov chain (provided it is unique) is a close approximation to the canonical measure, as well as being ergodic.

We will refer to such schemes by the name obtained by concatenating the names of each operator appearing in the ordering, using O instead of γC . For instance, the BAO scheme is given by the following update rule, which corresponds to applying the symplectic Euler scheme over one timestep, followed by one timestep of the Ornstein-Uhlenbeck stochastic flow (2.34).

Example 2 (BAO scheme). *The update rule is given by the following equations, where we introduce the intermediate momentum variable $p^{n+\frac{1}{2}}$:*

$$(2.37) \quad \begin{cases} p^{n+\frac{1}{2}} = p^n - \Delta t \nabla V(q^n) \\ q^{n+1} = q^n + \Delta t M^{-1} p^{n+\frac{1}{2}} \\ p^{n+1} = \alpha_{\Delta t} p^{n+\frac{1}{2}} + \sigma_{\Delta t} G^n, \end{cases}$$

where G^n is a standard dN -dimensional Gaussian.

Similarly, we define the BAOAB scheme.

Example 3 (BAOAB scheme). *The update rule is given by the following equations, with additional intermediate coordinate and momentum variables:*

$$(2.38) \quad \begin{cases} p^{n+\frac{1}{3}} = p^n - \frac{\Delta t}{2} \nabla V(q^n) \\ q^{n+\frac{1}{2}} = q^n + \frac{\Delta t}{2} M^{-1} p^{n+\frac{1}{3}} \\ p^{n+\frac{2}{3}} = \alpha_{\Delta t} p^{n+\frac{1}{3}} + \sigma_{\Delta t} G^n \\ q^{n+1} = q^{n+\frac{1}{2}} + \frac{\Delta t}{2} M^{-1} p^{n+\frac{2}{3}} \\ p^{n+1} = p^{n+\frac{2}{3}} - \frac{\Delta t}{2} \nabla V(q^{n+1}), \end{cases}$$

where, again, G^n is a standard dN -dimensional Gaussian.

Now we have a recipe to make an infinite number of numerical schemes, which can easily be implemented in a computer. We could even go further and consider methods with an uneven distribution for the secondary timesteps, the introduction of negative secondary timesteps for the A and B steps, and so on. This room for creativity highlights the need for criteria to assess the quality of such schemes. Several considerations have to be weighed.

- (i) Our aim is to compute long trajectories, which are needed to ensure that phase space is properly explored, as well as to obtain better statistical properties for averages (2.12). Thus, for a fixed computational budget, we desire a scheme which allows us to take as large a timestep Δt as possible. This is the issue of numerical stability.
- (ii) The use of a positive timestep Δt implies in general that the invariant measure for the Markov chain corresponding to a given scheme is not the canonical measure. This issue is called systematic error, or bias, and one would desire a scheme which minimizes this bias.
- (iii) The main computational cost in computing iterates of these numerical schemes is the evaluation of the gradient of the potential used for the B steps. As such, it is desirable to have a scheme which requires as few evaluations of this gradient per iteration. Some care must be taken when implementing these, to ensure that already computed gradients are not re-computed: for instance, the gradient in the last step of the BOAB scheme, is equal to the one in the first step of the next iteration.
- (iv) Notice that the parameter γ is free for the practitioner to choose. A natural question is to determine the properties of the marginal dynamics in q in the limit $\gamma \rightarrow +\infty$, and in particular if we obtain a consistent discretization of the overdamped Langevin dynamics.
- (v) Conversely, one could ask about properties of the dynamics as we take the Hamiltonian limit $\gamma \rightarrow 0$.

2.3.5 Error analysis for splitting schemes

Let us address the second of these concerns

2.3.6 Unbiased sampling

It turns out that one can devise schemes which have no systematic error: the Markov chain generating the trajectories has invariant measure exactly μ . These methods are based on the Metropolis-Hastings algorithm, which gives a general method to sample a given target distribution.

The Metropolis-Hastings algorithm

We aim to sample from a given target measure on \mathbb{R}^d . We suppose we have at our disposal a way to generate proposal points from a given point $\in \mathbb{R}^d$. This amounts to defining a transition kernel, the *proposal*, which we may take to be a map

$$T : \mathbb{R}^d \times \mathbb{R}^d \longrightarrow \mathbb{R}_+,$$

such that for any $x \in \mathbb{R}^d$, $T(x, \cdot)$ is a probability density on \mathbb{R}^d , and which is cheap to sample from (very often these are taken to be some form of Gaussian distribution). We also assume that we always have $T(x, y) > 0$. (This is always the case if the kernel is Gaussian). We also fix a function $r : \mathbb{R}_+ \rightarrow (0, 1]$, the *rule*, which satisfies the property

$$(2.39) \quad x \cdot r \left(\frac{1}{x} \right) = r(x)$$

We then define a Markov chain by iterating the following algorithm, starting from an arbitrary point $q^0 \in \mathbb{R}^d$.

Algorithm 1 (Metropolis-Hastings). *From a given point q^n*

(1) *Sample a proposal \tilde{q}^{n+1} according to the probability law $T(q^n, \cdot)$.*

(2) *Compute*

$$R(\tilde{q}^{n+1}, q^n) = r \left(\frac{\pi(\tilde{q}^{n+1})T(\tilde{q}^{n+1}, q^n)}{\pi(q^n)T(q^n, \tilde{q}^{n+1})} \right).$$

(3) *With probability $R(\tilde{q}^{n+1}, q^n)$, set $q^{n+1} = \tilde{q}^{n+1}$, otherwise, set $q^{n+1} = q^n$.*

(4) *Go back to step (1) with $q^n \leftarrow q^{n+1}$.*

Since T defines a Markov chain, we may always write $\tilde{q}^{n+1} = \Phi(q^n, \xi^n)$ for some family of *i.i.d.* variables $(\xi^n)_{n \geq 0}$. We can then write q^{n+1} in a concise form:

$$(2.40) \quad q^{n+1} = \Phi(q^n, \xi^n) + \mathbb{1}_{U^n > R(\Phi(q^n, \xi^n), q^n)} (q^n - \Phi(q^n, \xi^n)) = \Psi(q^n, \xi^n, U^n),$$

where the U^n are *i.i.d.* uniform on $[0, 1]$, such that the (ξ^n, U^n) are an independent family. This shows that the algorithm defines a Markov chain. Furthermore, we may compute

$$\begin{aligned} \pi(x)\mathbb{P}(q^1 = y | q^0 = x) &= \pi(x)T(x, y)R(x, y) \\ &= \pi(x)T(x, y)r \left(\frac{\pi(y)T(y, x)}{\pi(x)T(x, y)} \right) \\ (2.41) \quad &= \pi(y)T(y, x) \frac{\pi(x)T(x, y)}{\pi(y)T(y, x)} r \left(\frac{\pi(y)T(y, x)}{\pi(x)T(x, y)} \right) \\ &= \pi(y)T(y, x)r \left(\frac{\pi(x)T(x, y)}{\pi(y)T(y, x)} \right) \text{ (Using (2.39))} \\ &= \pi(y)\mathbb{P}(q^1 = x | q^0 = y). \end{aligned}$$

Thus, the chain is reversible with respect to π which is then an invariant measure. Note that the algorithm is applicable even when we do not know how to evaluate π , but only the ratios $\pi(x)/\pi(y)$, which is in particular the case for Gibbs measures.

Remark 6 (Rules for Metropolis-Hastings). *Possible choices for r are:*

1. *The Metropolis rule,*

$$r(x) = \min \{1, x\},$$

2. *The Barker rule,*

$$r(x) = \frac{x}{1+x},$$

3. *Any combination of these of the form, for $\gamma > 0$,*

$$r(x) = \frac{x}{1+x} \left(1 + 2 \left(\frac{1}{2} \min \left(r, \frac{1}{r} \right) \right)^\gamma \right).$$

Metropolized schemes for the underdamped Langevin dynamics

The Metropolis-Hastings algorithm provides a general recipe to define an unbiased Markov chain for the Langevin dynamics: one only needs to specify a proposition kernel and an acceptance rule. In fact,

Example 4 (A GHMC scheme). Suppose we have at our disposal i.i.d families $(U_n)_{n \geq 1}$ and $(G_n)_{n \geq 1}$ where U_1 is uniform on $[0, 1]$ and G_1 is a standard Gaussian in \mathbb{R}^{dN} .

$$(2.42) \quad \begin{cases} p^{n+\frac{1}{2}} = \alpha_{\Delta t} p^n + \sigma_{\Delta t} G_n \\ \tilde{p}^{n+\frac{1}{2}} = p^{n+\frac{1}{2}} - \frac{\Delta t}{2} \nabla V(q^n) \\ \tilde{q}^{n+1} = q^n + \Delta t M^{-1} \tilde{p}^{n+\frac{1}{2}} \\ \tilde{p}^{n+1} = \tilde{p}^{n+\frac{1}{2}} - \frac{\Delta t}{2} \nabla V(\tilde{q}^{n+1}) \\ r_n := \min \left\{ 1, \exp \left(-\beta (H(\tilde{q}^{n+1}, \tilde{p}^{n+1}) - H(q^n, p^{n+\frac{1}{2}})) \right) \right\} \\ (q^{n+1}, p^{n+1}) = \mathbb{1}_{U_n > r_n}(q^n, -p^{n+\frac{1}{2}}) + \mathbb{1}_{U_n \leq r_n}(\tilde{q}^{n+1}, \tilde{p}^{n+1}) \end{cases}$$

2.3.7 Asymptotic variance

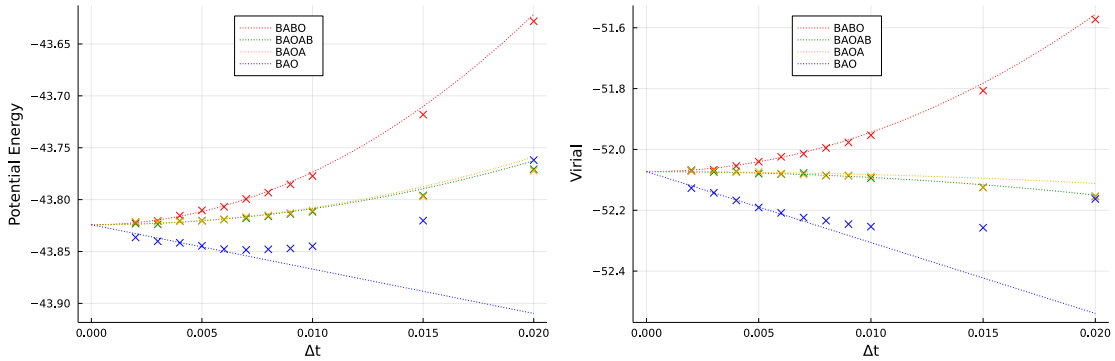


Figure 2.2: Effect of the time step on average potential energy and virial for a Lennard-Jones system of 27 particles.

To explain the overlap of bias between the BAOAB and the BAOA schemes observed for the potential energy and virial on Figure ??, we use the following result, which is a variation on the TU lemma.

Lemma 2. Let $P_{\Delta t}, Q_{\Delta t}$ be bounded operators on $B^\infty(\mathcal{E})$. Assume that, for any $n \geq 1$,

$$RP_{\Delta t}^n = Q_{\Delta t}^n S,$$

where R and S are bounded operators on $B^\infty(\mathcal{E})$, such that $R\mathbb{1} = \mathbb{1}$, and that the following ergodic condition holds: for any $\varphi \in B^\infty(\mathcal{E})$, and almost all $(q, p) \in \mathcal{E}$,

$$\lim_{n \rightarrow \infty} P_{\Delta t}^n \varphi(q, p) = \int_{\mathcal{E}} \varphi(q, p) \mu_{\Delta t, P}(dq, dp)$$

$$\lim_{n \rightarrow \infty} Q_{\Delta t}^n \varphi(q, p) = \int_{\mathcal{E}} \varphi(q, p) \mu_{\Delta t, Q}(dq, dp).$$

Then we can relate $\mu_{\Delta t, P}$ and $\mu_{\Delta t, Q}$ via the following relation:

$$(2.43) \quad \int_{\mathcal{E}} \varphi(q, p) \mu_{\Delta t, P}(dq, dp) = \int_{\mathcal{E}} S \varphi(q, p) \mu_{\Delta t, Q}(dq, dp)$$

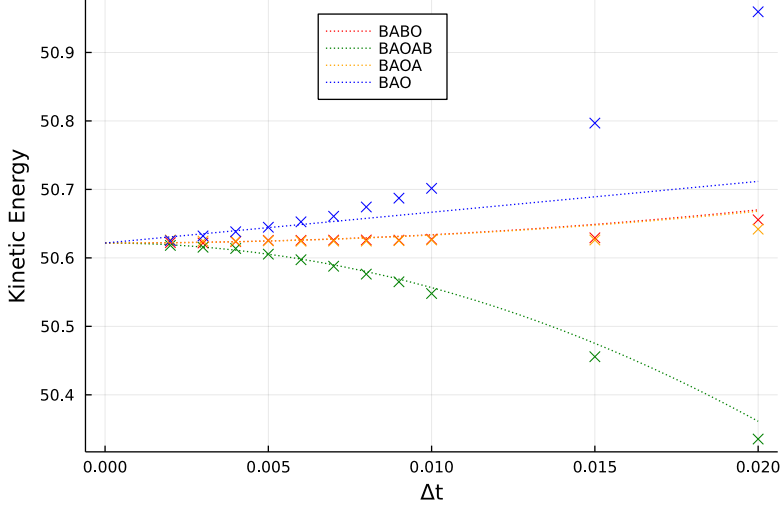


Figure 2.3: Effect of the time step on average kinetic energy for a Lennard-Jones system of 27 particles.

Proof. Fix an initial probability measure ρ on \mathcal{E} , absolutely continuous with respect to the Lebesgue measure. Then we may write, using dominated convergence to pass to the limit:

$$\begin{aligned}
& \int_{\mathcal{E}} RP_{\Delta t}^n \varphi(q, p) \rho(dq, dp) \\
&= \int_{\mathcal{E}} P_{\Delta t}^n \varphi(q, p) R^\dagger \rho(dq, dp) \\
&\xrightarrow{n \rightarrow \infty} \int_{\mathcal{E}} \left(\int_{\mathcal{E}} \varphi(q, p) \mu_{\Delta t, P}(dq, dp) \right) R^\dagger \rho(d\tilde{q}, d\tilde{p}) \\
&= \int_{\mathcal{E}} \varphi(q, p) \mu_{\Delta t, P}(dq, dp) \int_{\mathcal{E}} R \mathbb{1} d\rho \\
&= \int_{\mathcal{E}} \varphi(q, p) \mu_{\Delta t, P}(dq, dp)
\end{aligned}$$

Furthermore, applying the ergodic condition to the bounded function $S\varphi$ gives

$$\int_{\mathcal{E}} Q_{\Delta t}^n(S\varphi)(q, p) \rho(dq, dp) \xrightarrow{n \rightarrow \infty} \int_{\mathcal{E}} \left(\int_{\mathcal{E}} S\varphi(q, p) \mu_{\Delta t, Q}(dq, dp) \right) \rho(d\tilde{q}, d\tilde{p}) = \int_{\mathcal{E}} S\varphi(q, p) \mu_{\Delta t, Q}(dq, dp).$$

Since $RP_{\Delta t}^n = Q_{\Delta t}^n S$, identifying the two limits yields (2.43) \square

Corollary 1. Let $\pi_{\Delta t}^{\text{BAOA}}$ and $\pi_{\Delta t}^{\text{BAOAB}}$ be the invariant measures for the Markov transition operators defined respectively by the BAOA and BAOAB schemes for a fixed timestep Δt . If the ergodic condition holds, then the corresponding marginal distributions on \mathcal{D} are equal.

Proof. We denote by $P_{\Delta t}$ the transition operator for the BAOA scheme, and similarly $Q_{\Delta t}$ for the BAOAB scheme. It is straightforward to check that

$$e^{\frac{\Delta t}{2} B} P_{\Delta t}^n = Q_{\Delta t}^n e^{\frac{\Delta t}{2} B}.$$

Assuming the ergodic condition of Lemma 2 (TODO reference article for sufficient conditions), we can apply the result to get, for any bounded measurable observable φ ,

$$\int_{\mathcal{E}} \varphi(q, p) \pi_{\Delta t}^{\text{BAOA}}(dq, dp) = \int_{\mathcal{E}} e^{\frac{\Delta t}{2} B} \varphi(q, p) \pi_{\Delta t}^{\text{BAOAB}}(dq, dp).$$

Now if $\varphi(q, p) = \varphi(q, 0) := \varphi(q)$ for all p , then $e^{\frac{\Delta t}{2} B} \varphi = \varphi$, which yields the desired conclusion:

$$\forall \varphi \in B^\infty(\mathcal{D}), \int_{\mathcal{E}} \varphi(q) \pi_{\Delta t}^{\text{BAOA}}(dq, dp) = \int_{\mathcal{E}} \varphi(q) \pi_{\Delta t}^{\text{BAOAB}}(dq, dp).$$

□

The corollary also gives a non-trivial relation between the marginal distributions in momentum space, which explains the difference displayed on (Figure 2.3) between those two schemes.

2.3.8 Illustration: the equation of state of Argon

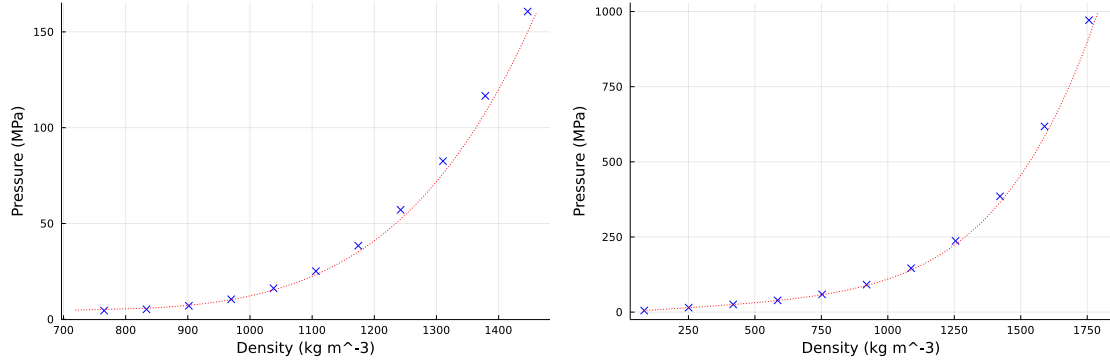


Figure 2.4: Simulated equations of state of Argon at 150 K (liquid phase, left) and 300 K (supercritical phase, right). Experimental reference curves are plotted in red, simulated data points are scattered in blue.

Chapter 3

Transport coefficients

3.1 Non-equilibrium dynamics

In the previous chapter, we investigated various numerical strategies to sample states from thermodynamic ensembles. The object now is to go beyond the computation of average observables, to consider dynamical behavior of molecular systems. One way to define question we may ask is how the system responds to small perturbations of the equilibrium. For instance we may think of applying a small non-gradient force ηF to the equilibrium force $-\nabla V(q)$, which amounts to considering the following equation:

$$(3.1) \quad \begin{cases} dq_t = M^{-1} p_t dt \\ dp_t = -\nabla V(q_t) dt + \eta F dt - \gamma M^{-1} p_t dt + \sqrt{\frac{2\gamma}{\beta}} dW_t \end{cases}$$

We can think of this as effectively tilting the potential landscape so that we expect the steady-state of this perturbed dynamics to feature a measurable flux of particles in the direction F , which we measure by looking at the average velocity in the direction F ,

$$(3.2) \quad \mathbb{E}_\eta [F \cdot (M^{-1} p)],$$

where \mathbb{E}_η denotes the average with respect to the steady-state for the dynamics (3.1), which we take to be a probability measure on \mathcal{E} , for which we have no closed form, in contrast to the equilibrium setting.

3.2 Linear response theory

3.3 Numerical schemes

Chapter 4

A Norton method

4.1 Introduction

So far, the non-equilibrium setting we considered was one in which we perturbed the dynamics by a constant forcing, and measured the linear relationship between the magnitude of the forcing and the induced response. An alternative idea would be to consider fixing the response, and measuring the magnitude of the forcing needed to induce it. This is the core of the Norton method.

4.2 Norton dynamics for the mobility observable

Let us fix a direction defined by a vector $F \in \mathbb{R}^{dN}$. The response we consider is the velocity in the direction F , which is the observable

$$F \cdot (M^{-1}p).$$

Again, we consider perturbed Langevin dynamics, but this time the magnitude of the non-gradient force η is replaced by a fluctuating magnitude Λ_t , which is determined in order to ensure that the response

$$v = F \cdot (M^{-1}p) = p \cdot (M^{-1}F)$$

is a constant.

4.2.1 The dynamics

Thus, we consider the dynamics

$$(4.1) \quad \begin{cases} dq_t = (M^{-1}p_t) dt \\ dp_t = -\nabla V(q_t)dt - \gamma (M^{-1}p_t) dt + \sqrt{\frac{2\gamma}{\beta}} dW_t + F d\Lambda_t, \end{cases}$$

where Λ_t is a real-valued stochastic process. We make the tacit assumption that for fixed v , the process Λ_t is well-defined and that ergodic averages

$$\frac{1}{T} \int_0^T d\Lambda_t = \frac{\Lambda_T - \Lambda_0}{T}$$

converge almost surely to some average value R_v under an invariant measure for the dynamics. We can easily write an equation for Λ_t , as follows. Our aim is to determine

$$\lim_{v \rightarrow 0} \frac{v}{R_v}$$

Using Itô's formula on the response, we get

$$(4.2) \quad d((M^{-1}F) \cdot p)_t = (M^{-1}F) \cdot \left(-\nabla V(q_t)dt - \gamma M^{-1}p_t dt + \sqrt{\frac{2\gamma}{\beta}} dW_t \right) + ((M^{-1}F) \cdot F) d\Lambda_t = 0,$$

which gives Λ_t as an Itô process,

$$(4.3) \quad d\Lambda_t = ((M^{-1}F) \cdot F)^{-1} (M^{-1}F) \cdot \left(\nabla V(q_t)dt + \gamma M^{-1}p_t dt - \sqrt{\frac{2\gamma}{\beta}} dW_t \right).$$

At this point, let us introduce the linear maps

$$(4.4) \quad \begin{aligned} P_{M,F} u &= \frac{(M^{-1}F) \cdot u}{(M^{-1}F) \cdot F} F \quad \forall u \in \mathbb{R}^{dN} \\ P_{M,F}^\perp &= \text{Id} - P_{M,F} \end{aligned}$$

which are simply the orthogonal projectors onto the subspace spanned by F and its orthogonal complement, with respect to the weighted scalar product

$$(4.5) \quad \langle x, y \rangle_M = \langle M^{-1}x, y \rangle.$$

Using this projector and substituting $d\Lambda_t$ for its value, we get the equation for the augmented dynamics $(q_t, p_t, \Lambda_t) \in \mathcal{E} \times \mathbb{R}$.

$$(4.6) \quad \begin{cases} dq_t = M^{-1}p_t dt \\ dp_t = P_{M,F}^\perp \left(-\nabla V(q_t)dt - \gamma M^{-1}p_t dt + \sqrt{\frac{2\gamma}{\beta}} dW_t \right) \\ d\Lambda_t = \frac{M^{-1}F}{(M^{-1}F) \cdot F} \cdot \left(\nabla V(q_t)dt + \gamma M^{-1}p_t dt - \sqrt{\frac{2\gamma}{\beta}} dW_t \right) \end{cases}$$

Notice this equation is almost the same as for the Langevin dynamics. The kinetic part is projected onto the F -subspace with respect to $\langle \cdot, \cdot \rangle_M$, and $d\Lambda_t$ is minus the coordinate in the F direction of the standard Langevin equation for dp_t , again with respect to $\langle \cdot, \cdot \rangle_M$. The Brownian motions W_t are the same in the last two equations, hence p_t and Λ_t are coupled processes.[GENERATOR FOR THE FULL DYNAMICS?]

$$(4.7) \quad \text{--- --- ---}$$

4.2.2 Analytic calculations for the kinetic dynamics

The kinetic part of the dynamics writes as the combination of a ballistic Hamiltonian evolution

$$(4.8) \quad \begin{cases} dq_t = 0 \\ dp_t = -P_{M,F}^\perp \nabla V(q_t) \end{cases} \implies \begin{cases} q_t = q_0 \\ p_t = p_0 - t P_{M,F}^\perp \nabla V(q_0) \end{cases}$$

and a fluctuation-dissipation part,

$$(4.9) \quad dp_t = -\gamma P_{M,F}^\perp M^{-1} p_t dt - \sqrt{\frac{2\gamma}{\beta}} P_{M,F}^\perp dW_t,$$

which can also be analytically solved. Indeed, applying Itô's formula to the rescaled process $e^{\gamma P_{M,F}^\perp M^{-1} t} p_t$ yields

$$e^{\gamma P_{M,F}^\perp M^{-1} t} \left(\gamma P_{M,F}^\perp M^{-1} p_t dt - \gamma P_{M,F}^\perp M^{-1} p_t dt - \sqrt{\frac{2\gamma}{\beta}} P_{M,F}^\perp dW_t \right),$$

hence we get

$$(4.10) \quad \begin{aligned} p_t &= e^{-\gamma P_{M,F}^\perp M^{-1} t} p_0 - \sqrt{\frac{2\gamma}{\beta}} \int_0^t e^{\gamma P_{M,F}^\perp M^{-1}(s-t)} P_{M,F}^\perp dW_s \\ &= e^{-\gamma P_{M,F}^\perp M^{-1} t} p_0 - \sqrt{\frac{2\gamma}{\beta}} \left(\int_0^t e^{-\gamma P_{M,F}^\perp M^{-1}s} P_{M,F}^\perp e^{-\gamma P_{M,F}^\perp M^{-1}s} ds \right)^{\frac{1}{2}} G, \end{aligned}$$

where the last equality holds in law if G is a standard dN -dimensional Gaussian, using Itô's isometry and the symmetry of $e^{\gamma P_{M,F}^\perp M^{-1} t}$ for all t . The matrix exponentials and integrals can be computed, however there is no concise expression like (2.20) because $P_{M,F}^\perp M^{-1}$ is not invertible.

In the case of a homogeneous system with $M = \alpha \text{Id}$ (in which case we can assume by a judicious choice of mass unit that $M = \text{Id}$), a more concise expression can be found, using the identity

$$e^{r\Pi} = \sum_{k=0}^{\infty} \frac{r^k}{k!} \Pi^k = \text{Id} + \left(\sum_{k=1}^{\infty} \frac{r^k}{k!} \right) \Pi = \text{Id} + (e^r - 1) \Pi.$$

This identity follows, for Π a linear projector, from applying the projector identity

$$\Pi = \Pi^2 = \Pi^3 = \dots$$

We write the following derivation in the case of a general projector Π , and conclude by taking the case $\Pi = P_{M,F}^\perp$. We also note $\Pi^\perp = \text{Id} - \Pi$.

$$(4.11) \quad \begin{aligned} e^{-\gamma \Pi t} p_0 - \sqrt{\frac{2\gamma}{\beta}} \Pi \left(\int_0^t e^{2\gamma s \Pi} ds \right)^{\frac{1}{2}} G &= (\text{Id} + (e^{-\gamma t} - 1) \Pi) p_0 - \sqrt{\frac{2\gamma}{\beta}} \Pi \left(\int_0^t (\text{Id} + (e^{-2\gamma s} - 1) \Pi) ds \right)^{\frac{1}{2}} G \\ &= (\Pi^\perp + e^{-\gamma t} \Pi) p_0 - \sqrt{\frac{2\gamma}{\beta}} \Pi \left(t \Pi^\perp + \frac{1 - e^{-2\gamma t}}{2\gamma} \Pi \right)^{\frac{1}{2}} G. \end{aligned}$$

Now, observe that \mathbb{R}^{dN} writes as the sum of two orthogonal spaces, each of which is an eigenspace for both Π and Π^\perp , and correspond respectively to the eigenvalues 0 and 1 (this correspondence being flipped upon passing from Π to Π^\perp). By an easy spectral calculation, we also have $\Pi^\alpha = \Pi$ for any $\alpha > 0$, which allows to conclude that

$$(a\Pi^\perp + b\Pi)^\alpha = a^\alpha \Pi^\perp + b^\alpha \Pi \quad \forall a, b, \alpha > 0,$$

and finally

$$(4.12) \quad \begin{aligned} e^{-\gamma \Pi t} p_0 - \sqrt{\frac{2\gamma}{\beta}} \Pi \left(\int_0^t e^{2\gamma s \Pi} ds \right)^{\frac{1}{2}} G &= \Pi^\perp p_0 + e^{-\gamma t} \Pi p_0 - \sqrt{\frac{2\gamma t}{\beta}} \Pi \Pi^\perp G - \sqrt{\frac{1 - e^{-2\gamma t}}{\beta}} \Pi G \\ &= \Pi^\perp p_0 + e^{-\gamma t} \Pi p_0 - \sqrt{\frac{1 - e^{-2\gamma t}}{\beta}} \Pi G, \end{aligned}$$

where we use $\Pi \Pi^\perp = 0$ for the last equality. Comparing equation (4.12) and equation (2.20) yields a clear interpretation of the action of the fluctuation-dissipation term on the dynamics: there is no effect in the direction tangent to F , and a standard Ornstein-Uhlenbeck process applies to the dynamics projected onto the subspace orthogonal to F (note ΠG can then be viewed as a $(dN - 1)$ -dimensional standard Gaussian by isotropy). We also note that a similar computation may be performed in the case where both M and $P_{M,F}$ are simultaneously diagonalizable, for instance if M is a diagonal matrix and F has a single non-zero component.

4.3 Splitting schemes

Consider the Norton dynamics on the state variable (q_t, p_t) . Its generator is given by the operator

$$(4.13) \quad \mathcal{L}_F \varphi(q, p) = (M^{-1}p) \cdot \nabla_q \varphi(q, p) - (P_{M,F}^\perp \nabla V(q) - \gamma P_{M,F}^\perp M^{-1}p) \cdot \nabla_p \varphi(q, p) - \frac{\gamma}{\beta} \text{Tr}(P_{M,F}^\perp \nabla_p^2 \varphi(q, p)),$$

which we rewrite as

$$(4.14) \quad \mathcal{L}_F = A + B_F + \gamma C_F, \quad \text{with} \quad \begin{cases} B_F \varphi(q, p) = (P_{M,F}^\perp \nabla V(q)) \cdot \nabla_p \varphi(q, p) \\ C_F \varphi(q, p) = -(P_{M,F}^\perp M^{-1}p) \cdot \nabla_p \varphi(q, p) + \frac{1}{\beta} \text{Tr}(P_{M,F}^\perp \nabla_p^2 \varphi(q, p)). \end{cases}$$

The A and B_F operators are the generators of exactly integrable dynamics (namely ballistic Hamiltonian dynamics), and C_F generates an analytically solvable diffusion process given in (4.10). Hence we can use a splitting scheme exactly as we did in the case of the Langevin dynamics, as discussed in section 2.3.4. We will use the exact same terminology in this context, referring to a scheme by the order in which the elementary dynamics are integrated. For instance, the BAO scheme associated with the Norton dynamics for F is the following. We fix a timestep $\Delta t > 0$.

Example 5 (Norton BAO scheme).

$$(4.15) \quad \begin{cases} p^{n+\frac{1}{2}} = p^n - \Delta t P_{M,F}^\perp \nabla V(q^n) \\ q^{n+1} = q^n + \Delta t M^{-1} p^{n+\frac{1}{2}} \\ p^{n+1} = e^{-\gamma P_{M,F}^\perp M^{-1} \Delta t} p^{n+\frac{1}{2}} - \sqrt{\frac{2\gamma}{\beta}} \left(\int_0^{\Delta t} e^{-\gamma P_{M,F}^\perp M^{-1} s} P_{M,F}^\perp e^{-\gamma P_{M,F}^\perp M^{-1} s} ds \right)^{\frac{1}{2}} G^n \end{cases}$$

The γC_F -step is cumbersome to write in full, but it is always of the form

$$p^{n+1} = R_{\Delta t} p^n + S_{\Delta t} G^n$$

for fixed matrices $R_{\Delta t}$ and $S_{\Delta t}$ which only have to be computed once.

4.4 Estimating transport coefficients

To estimate the transport coefficient ρ_F using this method, we need to estimate the average forcing. Recalling the SDE (4.6) for $d\Lambda$, the martingale term involving the Brownian motion cancels out under steady-state averaging. Hence we can estimate the average forcing using the following ergodic average:

$$(4.16) \quad \frac{1}{T} \int_0^T \frac{M^{-1} F}{(M^{-1} F) \cdot F} \cdot (\nabla V(q_t) + \gamma M^{-1} p_t) dt.$$

In the case of a mass matrix $M = m\text{Id}$ and $|F| = 1$, which we now assume on to lighten notation, this becomes

$$(4.17) \quad \frac{1}{T} \int_0^T F \cdot (\nabla V(q_t)) dt + \gamma v,$$

using the expression for the response, so that the finite difference estimator of ρ_F is given by

$$(4.18) \quad \widehat{\rho}_{F,T} = \frac{v}{\gamma v + \frac{1}{T} \int_0^T F \cdot (\nabla V(q_t)) dt}.$$

In practice, we approximate the continuous ergodic average in the denominator by discrete averages.

Appendix A

Implementation details

Appendix B

Study of the BAOA scheme

We consider time discretization schemes of underdamped Langevin dynamics known as the BAOA and BAOAB schemes, in order to compare the sampling bias induced by the timestep Δt for these two methods. Analysis of the timestep bias for the BAOAB scheme is given in [1], however it does not appear that the BAOA bias is so well understood. It has been observed numerically in [2] (Section III.B) that the bias on the kinetic marginal distribution is much lower using the BAOA method. We attempt to explain this from a theoretical point of view, before illustrating our results in numerical examples. Building on known results for the BAOAB scheme, we show the following results.

- (i) In section B.0.2, we express the invariant measure of the BAOA scheme in terms of the invariant measure of the BAOAB scheme (Proposition 7), and using this expression, we show, as in [2] (Section II.C), the equality between their respective configurational marginal distributions (Corollary 2).
- (ii) In section B.0.3, we show that the dominant error term for BAOA averages is only of order one in Δt , confirming that the BAOAB method is in general of higher order (Corollary 3).
- (iii) We show in section B.0.4 that for kinetic observables, however, the error is of second order in Δt , so that both marginal distributions are second-order accurate (Corollary 4).
- (iv) In section B.0.5, we give an expression for the dominant error term in the kinetic marginal distribution of the BAOA scheme (Proposition 8). In fact, we conjecture that, at least in dimension one, this term cancels, leading to an order of at least Δt^3 (Conjecture 1).
- (v) Lastly, in section B.0.6, we analyze the difference between the kinetic marginal distribution under the BAOA and BAOAB scheme (Proposition 9), and explain why this difference leads to a systematic underestimation of the kinetic variance in BAOAB trajectories (Remark 8).

B.0.1 Definitions and notations

The underdamped Langevin dynamics is defined by the following stochastic differential equation:

$$(B.1) \quad \begin{cases} dq_t = M^{-1} p_t dt, \\ dp_t = -\nabla V(q_t) dt - \gamma M^{-1} p_t dt + \sqrt{\frac{2\gamma}{\beta}} dW_t, \end{cases}$$

where $M \in \mathbb{R}^{dN \times dN}$ is a symmetric mass matrix, $(q_t, p_t) \in \mathcal{D} \times \mathbb{R}^{dN} := \mathcal{E}$, $(W_t)_{t \geq 0}$ is a standard dN -dimensional Brownian motion, and γ, β are positive real parameters, respectively the friction coefficient and the inverse temperature. \mathcal{D} is the configuration space, which is either the torus $(L(\mathbb{R}/\mathbb{Z}))^{dN}$ or the full space \mathbb{R}^{dN} .

The canonical measure, which we denote with the same symbol as its density,

$$(B.2) \quad \int_{\mathcal{E}} \varphi d\mu = \int_{\mathcal{E}} \varphi(q, p) \mu(q, p) dq dp = \frac{1}{Z} \int_{\mathcal{E}} \varphi(q, p) e^{-\beta(\frac{1}{2}p \cdot M^{-1}p + V(q))} dq dp$$

is invariant for this dynamics.

We can write μ as a product measure on $\mathbb{R}^{dN} \times \mathcal{D}$

$$(B.3) \quad \mu(q, p) = \kappa(p)\nu(q), \quad \nu(q) = Z_{\nu}^{-1} e^{-\beta V(q)}, \quad \kappa(p) = \det(2\pi\beta M^{-1})^{-\frac{1}{2}} e^{-\frac{\beta}{2}\langle M^{-1}p, p \rangle}.$$

Notice κ corresponds to a centered Gaussian law, the Maxwell-Boltzmann distribution. The generator of the Langevin dynamics is the operator

$$(B.4) \quad \mathcal{L}_{\gamma} = M^{-1}p \cdot \nabla_q - \nabla V(q) \cdot \nabla_p - \gamma M^{-1}p \cdot \nabla_p + \frac{\gamma}{\beta} \Delta_p,$$

which splits into three elementary generators, namely

$$\mathcal{L}_{\gamma} = A + B + \gamma C,$$

with

$$(B.5) \quad A = M^{-1}p \cdot \nabla_q, \quad B = -\nabla V(q) \cdot \nabla_p, \quad C = -M^{-1}p \cdot \nabla_p + \frac{1}{\beta} \Delta_p.$$

These generators give rise to dynamics which we can express explicitly, defined by the following evolution operators:

$$(B.6) \quad \begin{cases} e^{tA} \varphi(q, p) = \varphi(q + tM^{-1}p, p), \\ e^{tB} \varphi(q, p) = \varphi(q, p - t\nabla V(q)), \\ e^{t\gamma C} \varphi(q, p) = \mathbb{E} \left[\varphi \left(q, e^{-\gamma M^{-1}t} p + \sqrt{\frac{\gamma M^{-1}}{\beta} (1 - e^{-2M^{-1}t})} G \right) \right], \end{cases}$$

where G is a standard dN -dimensional Gaussian. The dynamics associated with the A and B part are deterministic Hamiltonian dynamics, and the C part gives rise to an Ornstein-Uhlenbeck process on momentum coordinates. We consider two splitting schemes for (B.1), as defined by the following evolution operators:

$$(B.7) \quad \begin{cases} P_{\Delta t} = e^{\Delta t B} e^{\frac{\Delta t}{2} A} e^{\Delta t \gamma C} e^{\frac{\Delta t}{2} A}, \\ Q_{\Delta t} = e^{\frac{\Delta t}{2} B} e^{\frac{\Delta t}{2} A} e^{\Delta t \gamma C} e^{\frac{\Delta t}{2} A} e^{\frac{\Delta t}{2} B}. \end{cases}$$

These correspond respectively to the BAOA and the BAOAB scheme. We also denote $\mu_{\Delta t, P}, \mu_{\Delta t, Q}$ the invariant measures for the Markov chains associated with (B.7). We assume these have smooth densities which we also denote $\mu_{\Delta t, P}, \mu_{\Delta t, Q}$, and that a certain ergodicity condition holds (see Lemma 1). Additionally we denote by $\nu_{\Delta t, P}, \nu_{\Delta t, Q}, \kappa_{\Delta t, P}, \kappa_{\Delta t, Q}$ the associated marginals and densities with obvious notation inspired by (B.3).

B.0.2 Relating invariant measures of discretization schemes

In this paragraph, we provide a formula for $\mu_{\Delta t, P}$ in terms of $\mu_{\Delta t, Q}$. This result allows one to very simply show the equality in the configurational marginals between these two measures, as noted in [2]. The main tool is the following result, which is a reformulation of the TU lemma (Lemma 9 from [1]).

Lemma 3. Let $P_{\Delta t}, Q_{\Delta t}$ be bounded operators on $B^\infty(\mathcal{E})$. Assume that, for any $n \geq 1$,

$$R_{\Delta t} P_{\Delta t}^n = Q_{\Delta t}^n S_{\Delta t},$$

where $R_{\Delta t}$ and $S_{\Delta t}$ are bounded operators on $B^\infty(\mathcal{E})$, such that $R_{\Delta t} \mathbb{1} = \mathbb{1}$, and that the following ergodic condition holds: for any $\varphi \in B^\infty(\mathcal{E})$, and almost all $(q, p) \in \mathcal{E}$,

$$\lim_{n \rightarrow \infty} P_{\Delta t}^n \varphi(q, p) = \int_{\mathcal{E}} \varphi(q, p) \mu_{\Delta t, P}(dq, dp)$$

$$\lim_{n \rightarrow \infty} Q_{\Delta t}^n \varphi(q, p) = \int_{\mathcal{E}} \varphi(q, p) \mu_{\Delta t, Q}(dq, dp).$$

Then we have the relation $\mu_{\Delta t, P}$ and $\mu_{\Delta t, Q}$ via the following relation:

$$\int_{\mathcal{E}} \varphi(q, p) \mu_{\Delta t, P}(dq, dp) = \int_{\mathcal{E}} (S_{\Delta t} \varphi)(q, p) \mu_{\Delta t, Q}(dq, dp)$$

Applying Lemma 1 to (B.7) yields the following result.

Proposition 7. The following relation between the densities $\mu_{\Delta t, P}$ and $\mu_{\Delta t, Q}$ holds.

$$(B.8) \quad \mu_{\Delta t, P}(q, p) = \mu_{\Delta t, Q} \left(q, p - \frac{\Delta t}{2} V(q) \right).$$

Proof. From the expressions (B.7), we immediately get:

$$(B.9) \quad P_{\Delta t}^n e^{\frac{\Delta t}{2} B} = e^{\frac{\Delta t}{2} B} Q_{\Delta t}^n,$$

whereby applying Lemma 1, we get for any test function φ ,

$$(B.10) \quad \int_{\mathcal{E}} e^{\frac{\Delta t}{2} B} \varphi d\mu_{P, \Delta t} = \int_{\mathcal{E}} \varphi d\mu_{Q, \Delta t}$$

Using equation (B.10) with $\psi = e^{-\frac{\Delta t}{2} B} \varphi$ yields an exact expression for $\mu_{\Delta t, P}$ in terms of $\mu_{\Delta t, Q}$:

$$(B.11) \quad \int_{\mathcal{E}} \varphi d\mu_{\Delta t, P} = \int_{\mathcal{E}} e^{-\frac{\Delta t}{2} B} \varphi d\mu_{\Delta t, Q}.$$

Since φ is arbitrary, we infer that at the level of densities,

$$(B.12) \quad \mu_{\Delta t, P}(q, p) = \left(e^{-\frac{\Delta t}{2} B} \right)^\dagger \mu_{\Delta t, Q}(q, p),$$

where \dagger denotes the adjoint on the flat space $L^2(\mathcal{E})$. A simple computation shows that

$$e^{-\frac{\Delta t}{2} B^\dagger} = e^{\frac{\Delta t}{2} B},$$

since $B^\dagger = -B$. Hence,

$$(B.13) \quad \mu_{\Delta t, P}(q, p) = e^{\frac{\Delta t B}{2}} \mu_{\Delta t, Q}(q, p) = \mu_{\Delta t, Q} \left(q, p - \frac{\Delta t}{2} \nabla V(q) \right),$$

which is the desired conclusion. \square

Relation (B.13) is enough to show an equality between the configurational marginal distributions $\nu_{\Delta t, P}$ and $\nu_{\Delta t, Q}$, as noted in [2].

Corollary 2. *The marginal distributions in the q variable of $\mu_{\Delta t, P}$ and $\mu_{\Delta t, Q}$ coincide:*

$$(B.14) \quad \nu_{\Delta t, Q}(q) = \nu_{\Delta t, P}(q).$$

Proof. Write, for any $q \in \mathcal{D}$,

$$\begin{aligned} \nu_{\Delta t, Q}(q) &= \int_{\mathbb{R}^{dN}} \mu_{\Delta t, Q}(q, p) dp \\ &= \int_{\mathbb{R}^{dN}} \mu_{\Delta t, Q}\left(q, p - \frac{\Delta t}{2} \nabla V(q)\right) dp \\ &= \int_{\mathbb{R}^{dN}} \mu_{\Delta t, P}(q, p) dp \\ &= \nu_{\Delta t, P}(q), \end{aligned}$$

which proves the claim. \square

B.0.3 Error estimate on the phase space measure

We now turn to obtaining the dominant order in the sampling bias of $\mu_{\Delta t, P}$, building on previously known results for $\mu_{\Delta t, Q}$, and the relation (B.8). Error estimates on $\mu_{\Delta t, Q}$ have been investigated in [1] (Section 1.4). In particular, the following expansion of $\mu_{\Delta t, Q}$ is derived, which will be central in our analysis.

Theorem 1 (Theorem 13 in [1]). *There exists a smooth function f_2 such that for any smooth ψ ,*

$$(B.15) \quad \int_{\mathcal{E}} \psi(q, p) \mu_{\Delta t, Q}(q, p) dq dp = \int_{\mathcal{E}} \psi(q, p) \mu(q, p) dq dp + \Delta t^2 \int_{\mathcal{E}} \varphi(q, p) f_2(q, p) \mu(q, p) dq dp + \Delta t^4 r_{\psi, \gamma, \Delta t},$$

where the remainder $r_{\psi, \gamma, \Delta t}$ is uniformly bounded for Δt sufficiently small. Moreover, an expression for the dominant error term is obtained,

$$(B.16) \quad \begin{cases} f_2 = \tilde{f}_2 - \frac{1}{8}(A + B)g \\ \mathcal{L}_\gamma^* \tilde{f}_2 = \frac{1}{12}(A + B) \left[\left(A + \frac{B}{2} \right) g \right], \\ g := \beta(M^{-1}p) \cdot \nabla V(q) \end{cases}$$

where \mathcal{L}_γ^* is the adjoint of \mathcal{L}_γ on the weighted space $L^2(\mu)$.

Smoothness here is meant in a technical sense (see Definition 8 in [1]), which we refrain from detailing here. Using this expansion, one can derive the dominant order error for the BAOA scheme.

Corollary 3. *For any smooth observable φ ,*

$$(B.17) \quad \int_{\mathcal{E}} \varphi(q, p) \mu_{\Delta t, P}(q, p) dq dp = \int_{\mathcal{E}} \varphi(q, p) \left(1 + \frac{\Delta t}{2} g(q, p) \right) \mu(q, p) dq dp + O(\Delta t^2),$$

where g is given by (B.16).

Proof. Combining (B.15) with (B.8), we get the following estimation for averages with respect to $\mu_{\Delta t, P}$:

$$(B.18) \quad \int_{\mathcal{E}} \varphi(q, p) \mu_{\Delta t, P}(q, p) dq dp = \int_{\mathcal{E}} \varphi(q, p) \mu \left(q, p - \frac{\Delta t}{2} \nabla V(q) \right) dq dp + O(\Delta t^2).$$

Taylor expanding μ gives

$$\mu\left(q, p - \frac{\Delta t}{2} \nabla V(q)\right) = \mu(q, p) \left(1 + \frac{\Delta t}{2} \beta(M^{-1}p) \cdot \nabla V(q) + O(\Delta t^2)\right) = \mu(q, p) \left(1 + \frac{\Delta t}{2} g(q, p) + O(\Delta t^2)\right),$$

hence we get

$$(B.19) \quad \int_{\mathcal{E}} \varphi(q, p) \mu_{\Delta t, P}(q, p) dq dp = \int_{\mathcal{E}} \varphi(q, p) \mu(q, p) \left(1 + \frac{\Delta t}{2} g(q, p) + O(\Delta t^2)\right) dq dp,$$

which proves the claim. \square

B.0.4 Error estimates on the kinetic marginal distributions

Equation (B.17) expresses the fact that the invariant measure $\mu_{\Delta t, P}$ is only exact at first order in Δt , which is one less than $\mu_{\Delta t, Q}$. So in full generality, one can expect an error of order Δt on averages obtained from BAOA trajectories, versus Δt^2 for averages computed from BAOAB trajectories. However, if we restrict ourselves to marginal observables, that is observables which only depend on the configurational coordinate or the kinetic coordinate, the first order error term vanishes. Indeed, we have the following.

Corollary 4. *Let $\varphi(q, p) = \varphi(q)$ or $\varphi(q, p) = \varphi(p)$ be a marginal observable. Then*

$$\int_{\mathcal{E}} \varphi d\mu_{\Delta t, P} = \int_{\mathcal{E}} \varphi d\mu + O(\Delta t^2).$$

Proof. By (B.17), it is sufficient to show

$$(B.20) \quad \int_{\mathcal{E}} \varphi g d\mu = 0.$$

This follows from the following cancellations.

$$(B.21) \quad \int_{\mathbb{R}^{dN}} g(q, p) \mu(q, p) dp = \int_{\mathcal{D}} g(q, p) \mu(q, p) dq = 0.$$

Indeed,

$$\int_{\mathbb{R}^{dN}} \beta(M^{-1}p) \cdot \nabla V(q) \mu(q, p) dp = 0,$$

since the integrand is an odd function of p , and the marginal of μ in p is a centered Gaussian density. Also,

$$\int_{\mathcal{D}} \beta(M^{-1}p) \cdot \nabla V(q) \mu(q, p) dq = - \int_{\mathcal{D}} (M^{-1}p) \cdot \nabla_q \mu(q, p) dq = 0,$$

by an integration by parts. By first integrating (B.20) over the coordinate independent of φ , one of the cancellations (B.21) yields the result. \square

Corollary 2 gives no new information concerning configurational observables, since we already know by Corollary 1 that these have the same averages under $\mu_{\Delta t, P}$ and $\mu_{\Delta t, Q}$, and that by Theorem 1, these have error of order Δt^2 . However, kinetic observables may yield different averages.

B.0.5 Analysis of the second order error term for kinetic averages under $\mu_{\Delta t, P}$

It was observed numerically in [2] that the averages of the kinetic and configurational temperatures computed with a BAOA scheme have a bias of order greater than Δt , as expected from the argument above. In fact, for the kinetic temperature, the order appears to be greater than Δt^2 , in contrast to averages computed with the BAOAB method. Understanding this behavior theoretically requires comparing second order error terms.

We show the following result, which identifies the second-order error term for kinetic observables.

Proposition 8. *Let $\psi(q, p) = \psi(p)$ be a smooth kinetic observable. Then,*

$$(B.22) \quad \int_{\mathcal{E}} \psi(p) \mu_{\Delta t, P}(q, p) dq dp = \int_{\mathcal{E}} \psi(p) \mu(q, p) dp dq + \Delta t^2 \int_{\mathcal{E}} \psi(p) \tilde{f}_2(q, p) \mu(q, p) dq dp + O(\Delta t^3),$$

where \tilde{f}_2 is given by (B.16).

From Theorem 13 of [1], this error term is identical to the dominant error term for OBABO averages, and minus the dominant error term for OABAO averages.

Proof. By writing

$$\int_{\mathcal{E}} \psi(q, p) \mu_{\Delta t, P}(q, p) dq dp - \int_{\mathcal{E}} \psi(q, p) \mu(q, p) dp dq = \int_{\mathcal{E}} \left(\psi(q, p) - \int_{\mathcal{E}} \psi dq \right) \mu_{\Delta t, P}(q, p) dq dp,$$

we may assume without loss of generality that ψ has average 0 with respect to μ .

Using (B.15), we get

$$\int_{\mathcal{E}} \psi(p) \mu_{\Delta t, Q}(q, p) dq dp = \Delta t^2 \int_{\mathcal{E}} \psi(p) f_2(q, p) \mu(q, p) dq dp + O(\Delta t^3),$$

so that using our relation (B.8), we get

$$\int_{\mathcal{E}} \psi(p) \mu_{\Delta t, P}(q, p) dq dp = \int_{\mathcal{E}} \psi(p) e^{\frac{\Delta t}{2} B} \mu(q, p) dq dp + \Delta t^2 \int_{\mathcal{E}} \psi(p) e^{\frac{\Delta t}{2} B} [f_2(q, p) \mu(q, p)] dq dp + O(\Delta t^3).$$

This rewrites, at dominant order,

$$\int_{\mathcal{E}} \psi(p) \mu \left(q, p - \frac{\Delta t}{2} \nabla V(q) \right) dq dp + \Delta t^2 \int_{\mathcal{E}} \psi(p) f_2(q, p) \mu(q, p) dq dp + O(\Delta t^3).$$

Expanding μ to the second order yields

$$\begin{aligned} & \mu \left(q, p - \frac{\Delta t}{2} \nabla V(q) \right) + O(\Delta t^3) \\ &= \mu(q, p) \left[1 + \beta \frac{\Delta t}{2} (M^{-1} p) \cdot \nabla V(q) + \frac{\Delta t^2}{8} [(\beta M^{-1} p) \otimes (\beta M^{-1} p) \nabla V(q)] \cdot \nabla V(q) - \beta \frac{\Delta t^2}{8} (M^{-1} \nabla V(q)) \cdot \nabla V(q) \right] \\ &= \mu(q, p) \left[1 + \beta \frac{\Delta t}{2} (M^{-1} p) \cdot \nabla V(q) + \frac{\Delta t^2}{8} (g^2(q, p) - \beta (M^{-1} \nabla V(q)) \cdot \nabla V(q)) \right]. \end{aligned}$$

Using $\int \psi d\mu = 0$ and the cancellation (B.21) on q to remove the first order term, we obtain:

$$(B.23) \quad \int_{\mathcal{E}} \psi(p) \mu_{\Delta t, P}(q, p) dq dp = \Delta t^2 \int_{\mathcal{E}} \psi(p) \left(\frac{1}{8} (g^2(q, p) - \beta (M^{-1} \nabla V(q)) \cdot \nabla V(q)) + f_2(q, p) \right) \mu(q, p) dq dp + O(\Delta t^3).$$

Simplifications are possible. First, observe that

$$-\beta(M^{-1}\nabla V(q)) \cdot \nabla V(q) = Bg(q, p),$$

so that, using the expression for f_2 given in (B.16), we get

$$(B.24) \quad \int_{\mathcal{E}} \psi(p) \mu_{\Delta t, P}(q, p) dq dp = \Delta t^2 \int_{\mathcal{E}} \psi(p) \left(\frac{1}{8} (g^2(q, p) - Ag(q, p)) + \tilde{f}_2(q, p) \right) \mu(q, p) dq dp + O(\Delta t^3).$$

Next, we examine the term

$$(g^2(q, p) - Ag(q, p)) \mu(q, p) = [\beta^2 ((M^{-1}p) \cdot \nabla V(q))^2 - \beta(M^{-1}p) \cdot (\nabla^2 V(q) M^{-1}p)] \mu(q, p),$$

by a straightforward calculation, where ∇^2 denotes the Hessian matrix. This expression is a finite sum of diagonal terms coming from both terms inside the brackets, and off-diagonal terms coming only from the rightmost term inside the bracket. Importantly, these all vanish when integrated against the configurational marginal of μ . To make this precise, we index p and q as

$$p = (p_i)_{1 \leq i \leq dN}, \quad q = (q_i)_{1 \leq i \leq dN}.$$

Fixing indices $i \neq j$, the diagonal term corresponding to i is

$$(B.25) \quad \left[\beta^2 (M^{-1}p)_i^2 \left(\frac{\partial}{\partial q_i} V(q) \right)^2 - \beta (M^{-1}p)_i^2 \frac{\partial^2}{\partial q_i^2} V(q) \right] \mu(q, p) = (M^{-1}p)_i^2 \frac{\partial^2}{\partial q_i^2} \mu(q, p),$$

and the off-diagonal term corresponding to (i, j) is

$$(B.26) \quad -\beta (M^{-1}p)_i (M^{-1}p)_j \frac{\partial}{\partial q_i} V(q) \frac{\partial}{\partial q_j} V(q) \mu(q, p) = -\frac{1}{\beta} (M^{-1}p)_i (M^{-1}p)_j \frac{\partial^2}{\partial q_i \partial q_j} \mu(q, p).$$

Factoring out the q -independent terms, and using the cancellations

$$(B.27) \quad \int_{\mathcal{D}} \frac{\partial^2}{\partial q_i^2} \mu(q, p) dq = \int_{\mathcal{D}} \frac{\partial^2}{\partial q_i \partial q_j} \mu(q, p) dq = 0,$$

which follow by integration by parts, we infer

$$(B.28) \quad \int_{\mathcal{E}} \psi(p) \mu_{\Delta t, P}(q, p) dq dp = \Delta t^2 \int_{\mathcal{E}} \psi(p) \tilde{f}_2(q, p) \mu(q, p) dq dp + O(\Delta t^3),$$

which concludes the proof. \square

Remark 7. Using exponential decay estimates on the evolution semigroup $(e^{t\mathcal{L}_\gamma})_{t \geq 0}$, (see [1], paragraph 1.1.1 and references therein for more detail) one can show that the inverse operator \mathcal{L}_γ^{-1} is well-defined for smooth centered observables. Thus $\mathcal{L}_\gamma^{-1}\psi$ is well defined, say $\mathcal{L}_\gamma\Psi(q, p) = \psi(p)$. Hence, (B.22) rewrites

$$\begin{aligned} \int_{\mathcal{E}} \psi(p) \mu_{\Delta t, P}(q, p) dq dp &= \Delta t^2 \int_{\mathcal{E}} \mathcal{L}_\gamma\Psi(q, p) \tilde{f}_2(q, p) \mu(q, p) dq dp + O(\Delta t^3) \\ &= \Delta t^2 \int_{\mathcal{E}} \Psi(q, p) \mathcal{L}_\gamma^* \tilde{f}_2(q, p) \mu(q, p) dq dp + O(\Delta t^3) \\ &= \frac{\Delta t^2}{12} \int_{\mathcal{E}} \Psi(q, p) \left[(A + B) \left(A + \frac{B}{2} \right) g \right] (q, p) \mu(q, p) dq dp + O(\Delta t^3), \end{aligned}$$

using (B.16), which provides an alternative expression for the dominant error term. Numerical evidence (see Figure B.11) suggests that the error on BAOA and BAOAB averages is at dominant order independent of γ . Since the error term on BAOA given in (B.22) depends on γ , this suggests that this term is zero, motivating the following conjecture.

Conjecture 1. For any smooth centered kinetic observable $\psi(p)$, we have

$$(B.29) \quad \int_{\mathcal{E}} (\mathcal{L}_\gamma^{-1} \psi)(q, p) \left[(A + B) \left(A + \frac{B}{2} \right) g \right] (q, p) \mu(q, p) dq dp = 0.$$

This would in particular imply that the kinetic marginal $\kappa_{\Delta t, P}$ is correct at order at least three in Δt , and is the subject of further investigation.

B.0.6 Analysis of the discrepancy between the dominant error terms on the kinetic marginals.

Numerical evidence presented in [2] shows a significant discrepancy between $\kappa_{\Delta t, P}$ and $\kappa_{\Delta t, Q}$. Specifically, $\kappa_{\Delta t, Q}$ in the case $d = N = 1$ tends to present a sharper peak than $\kappa_{\Delta t, P}$, thus underestimating the variance in the kinetic marginal. We show this in this paragraph this behavior is generic, in the sense that it does not, up to a shape parameter, depend on V . The arguments above show that

$$(B.30) \quad \begin{aligned} \int_{\mathcal{E}} \psi(p) \mu_{\Delta t, P}(q, p) dq dp &= \int_{\mathbb{R}^{dN}} \psi(p) \kappa_{\Delta t, P}(p) dp \\ &= \int_{\mathbb{R}^{dN}} \psi(p) \kappa(p) dp + \Delta t^2 \int_{\mathbb{R}^{dN}} \psi(p) \left(\int_{\mathcal{D}} \tilde{f}_2(q, p) \nu(q) dq \right) \kappa(p) dp + O(\Delta t^3), \end{aligned}$$

where we used the product form (B.3) for μ . Similarly,

$$(B.31) \quad \int_{\mathcal{E}} \psi(p) \kappa_{\Delta t, Q}(p) dp = \int_{\mathbb{R}^{dN}} \psi(p) \kappa(p) dp + \Delta t^2 \int_{\mathbb{R}^{dN}} \psi(p) \left(\int_{\mathcal{D}} f_2(q, p) \nu(q) dq \right) \kappa(p) dp + O(\Delta t^3),$$

so that

$$\begin{aligned} \int_{\mathcal{E}} \psi(p) (\kappa_{\Delta t, P}(p) - \kappa_{\Delta t, Q}(p)) dp &= \Delta t^2 \int_{\mathbb{R}^{dN}} \psi(p) \left(\int_{\mathcal{D}} (\tilde{f}_2(q, p) - f_2(q, p)) \nu(q) dq \right) \kappa(p) dp + O(\Delta t^3) \\ &= \frac{\Delta t^2}{8} \int_{\mathbb{R}^{dN}} \psi(p) \left(\int_{\mathcal{D}} (A + B) g(q, p) \nu(q) dq \right) \kappa(p) dp + O(\Delta t^3). \end{aligned}$$

Hence at the level of densities, we have at dominant order,

$$\kappa_{\Delta t, P}(p) - \kappa_{\Delta t, Q}(p) = \frac{\Delta t^2 \kappa(p)}{8} \int_{\mathcal{D}} (A + B) g(q, p) \nu(q) dq + O(\Delta t^3),$$

using the expressions for f_2 and \tilde{f}_2 given in (B.16). The following proposition gives an alternative expression for this discrepancy term.

Proposition 9. We have the following expression for the discrepancy term.

$$(B.32) \quad \kappa_{\Delta t, P}(p) - \kappa_{\Delta t, Q}(p) = \frac{\Delta t^2}{8} \text{Tr} \left(\left((\beta M^{-1} p)^{\otimes 2} - \beta M^{-1} \right)^\top \text{Cov}_\nu(\nabla V) \right) \kappa(p) + O(\Delta t^3).$$

Proof. For simplicity we assume $Z_\nu = \frac{\Delta t^2}{8} = \kappa(p) = 1$. This has no incidence on our computations. We write:

$$(B.33) \quad (A + B) g(q, p) \nu(q) = \beta \left[(M^{-1} p) \cdot (\nabla^2 V(q) M^{-1} p) - (M^{-1} \nabla V(q)) \cdot \nabla V(q) \right] e^{-\beta V(q)}.$$

Setting $\tilde{p} = M^{-1} p$, we get

$$(B.34) \quad (A + B)g(q, M\tilde{p})\nu(q) = \beta [\tilde{p} \cdot (\nabla^2 V(q)\tilde{p}) - (M^{-1}\nabla V(q)) \cdot \nabla V(q)] e^{-\beta V(q)}.$$

This is a sum of terms of the form

$$T_{ij}(q, p) = \left[\beta \tilde{p}_i \tilde{p}_j \frac{\partial^2}{\partial q_i \partial q_j} V(q) - \beta M_{i,j}^{-1} \frac{\partial}{\partial q_i} V(q) \frac{\partial}{\partial q_j} V(q) \right] e^{-\beta V(q)}.$$

Upon integrating this term over \mathcal{D} , we can integrate the left-most term by parts (boundary terms cancel out by periodicity or by growth conditions on V), to obtain

$$\int_{\mathcal{D}} T_{ij}(q, p) dq = \int_{\mathcal{D}} \left[\beta^2 \tilde{p}_i \tilde{p}_j \frac{\partial}{\partial q_i} V(q) \frac{\partial}{\partial q_j} V(q) - \beta M_{i,j}^{-1} \frac{\partial}{\partial q_i} V(q) \frac{\partial}{\partial q_j} V(q) \right] e^{-\beta V(q)} dq.$$

Hence,

$$\int_{\mathcal{D}} T_{ij}(q, p) dq = (\beta^2 \tilde{p}_i \tilde{p}_j - \beta M_{i,j}^{-1}) \int_{\mathcal{D}} \frac{\partial}{\partial q_i} V(q) \frac{\partial}{\partial q_j} V(q) e^{-\beta V(q)} dq,$$

so that

$$\int_{\mathcal{D}} (A + B)g(q, p)\nu(q) dq = \sum_{i,j} (\beta^2 \tilde{p}_i \tilde{p}_j - \beta M_{i,j}^{-1}) \int_{\mathcal{D}} \frac{\partial}{\partial q_i} V(q) \frac{\partial}{\partial q_j} V(q) e^{-\beta V(q)} dq,$$

which we rewrite

$$(B.35) \quad \left((\beta M^{-1}p)^{\otimes 2} - \beta M^{-1} \right) : \int_{\mathcal{D}} (\nabla V \otimes \nabla V)(q)\nu(q) dq = \text{Tr} \left(\left((\beta M^{-1}p)^{\otimes 2} - \beta M^{-1} \right)^{\top} \text{Cov}_{\nu}(\nabla V) \right),$$

using the fact that ∇V is a centered observable with respect to ν , and concluding the proof. \square

Remark 8. This expression for the discrepancy term is not particularly wieldy, however it does explain the behavior observed in [2]. In the case $d = N = \beta = M = 1$, it becomes,

$$\kappa_{\Delta t, P}(p) - \kappa_{\Delta t, Q}(p) = \frac{\Delta t^2}{8} (p^2 - 1) \text{Var}_{\nu}(V') \kappa(p) + O(\Delta t^3),$$

which is, up to a constant, the same correction term for any potential V . We plot this correction profile in figure B.1. The shape of this profile explains the higher peak observed in $\kappa_{\Delta t, Q}$.

B.1 Numerical results

We propose illustrating our computations with numerical examples, on toy one dimensional systems.

- (i) In section B.1.1, we define the potentials used for all the following experiments, and describe the sampling method used.
- (ii) In section B.1.2, we verify numerically the relation (B.14).
- (iii) In section B.1.3, we show that there is a significant discrepancy between the two kinetic marginal distributions. We also pinpoint the main, and possibly only source of this error, namely the γ -independent term (B.32).
- (iv) In section B.1.4, we numerically verify that the first order behavior (B.19) is correct.
- (v) In section B.1.5, we give an explicit example of an observable for which the BAOA scheme yields a bias of order Δt .
- (vi) Finally, in section B.1.6, we show that the effect of the parameter γ is undetectable at the level of the kinetic marginals, motivating Conjecture 1.

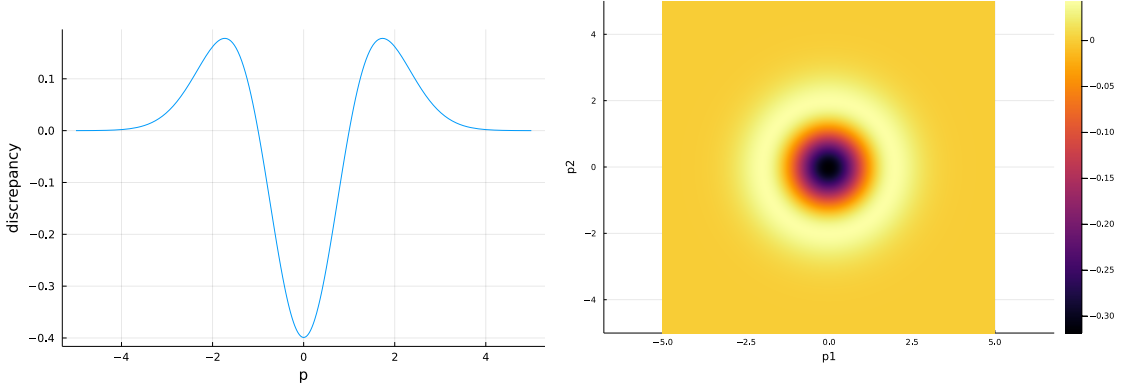


Figure B.1: Profile of the discrepancy term in one and two dimension, in the case of identity covariances for ∇V .

B.1.1 Models

We take $\beta = 1$, $M = \text{Id}$, and consider four potentials:

- Periodic potential

$$\mathcal{D} = L(\mathbb{R}/\mathbb{Z}), \quad L = 1, \quad V(q) = \sin(2\pi q/L),$$

- Quadratic potential

$$\mathcal{D} = \mathbb{R}, \quad V(q) = \alpha \frac{q^2}{2}, \quad \alpha = 1,$$

- Double well potential

$$\mathcal{D} = \mathbb{R}, \quad V(q) = \alpha \frac{q^2}{2} + \beta e^{-\frac{q^2}{2\sigma^2}}, \quad \alpha = 1, \quad \beta = 4, \quad \sigma = 0.5,$$

- Tilted double well potential

$$\mathcal{D} = \mathbb{R}, \quad V(q) = \alpha \frac{q^2}{2} + \gamma q + \beta e^{-\frac{q^2}{2\sigma^2}}, \quad \alpha = 1, \quad \beta = 4, \quad \gamma = 1, \quad \sigma = 0.5.$$

Analytically unknown normalizing constants and reference quantities were obtained through numerical integration of μ , using trapezoid rules with a mesh size of 10^{-6} . For unbounded coordinates, we truncated the domain to the interval $[-5, 5]$. Approximations of $\mu_{\Delta t, P}, \mu_{\Delta t, Q}$ were computed by recording the states of 10,000 independently evolving trajectories over 2×10^6 timesteps in a 1000×1000 two-dimensional histogram on the truncated domain. The rare sample points outside of the truncated domain were discarded.

B.1.2 Equality of marginal configurational distributions

On Figures B.2 and B.3, we verify numerically the equality (B.14) between the configurational marginal distributions $\nu_{\Delta t, Q}$ and $\nu_{\Delta t, P}$, which holds for any Δt . This point was demonstrated in [2].

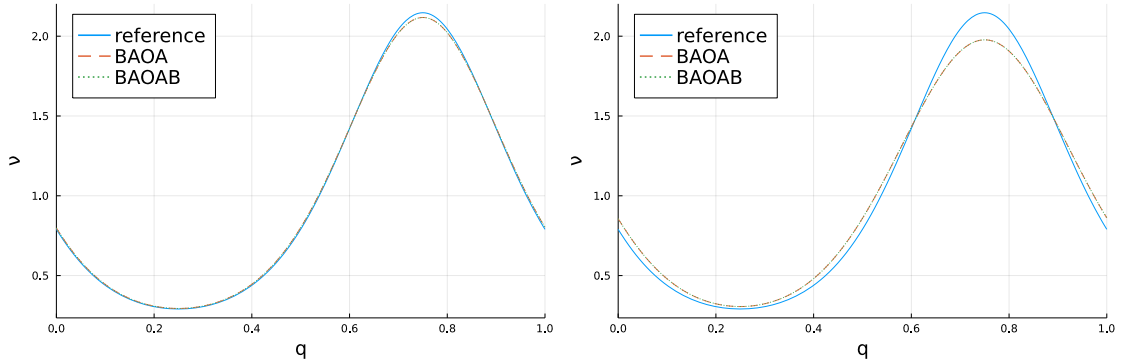


Figure B.2: Marginal configurational distributions for the periodic potential. Left: $\Delta t = 0.1$. Right: $\Delta t = 0.2$. Even for large timesteps, the distributions coincide perfectly.

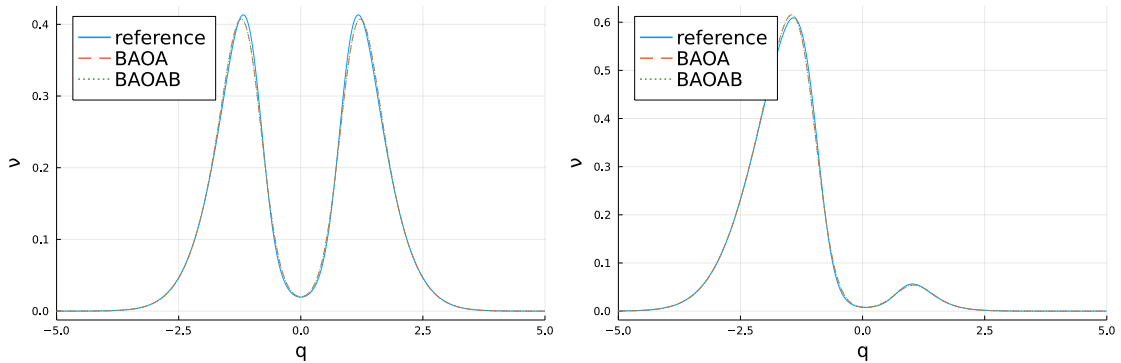


Figure B.3: Marginal configurational distributions for $\Delta t = 0.4$. Left: double well potential. Right: tilted double well potential.

B.1.3 Comparison of marginal kinetic distributions

We observe, as in [2], that the kinetic marginal distribution $\kappa_{\Delta t, Q}$ departs from the reference at a faster rate than $\kappa_{\Delta t, P}$, and more precisely appears to underestimate the variance, leading to a sharper distribution. Additionally we observe that removing the part of the bias on BAOAB due to the discrepancy term (B.32) leads to a significant improvement. These corrected marginals are plotted under the label "correction". See Figures B.4 and B.5.

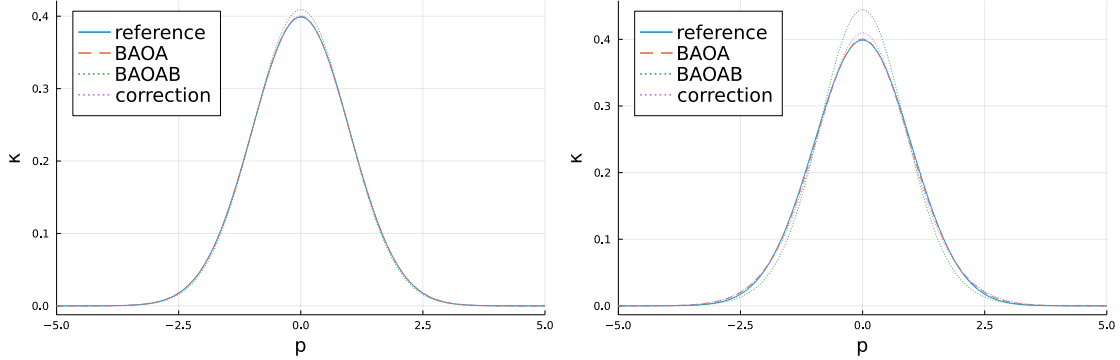


Figure B.4: Marginal kinetic distributions for the periodic potential. Left: $\Delta t = 0.1$. Right: $\Delta t = 0.2$.

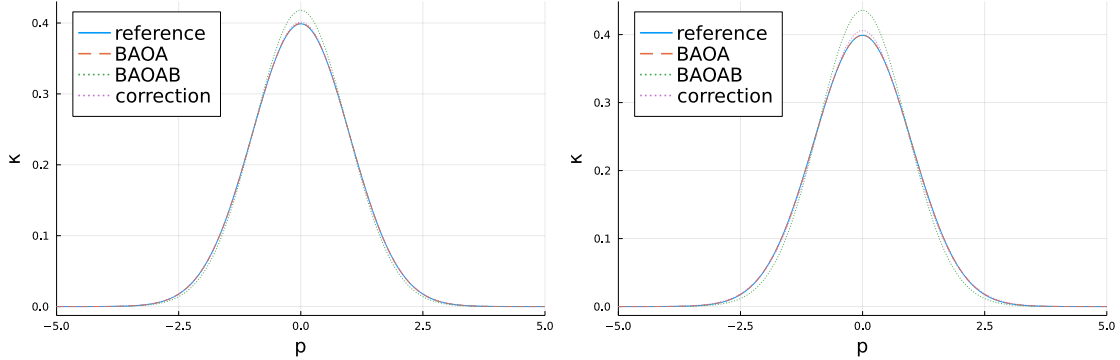


Figure B.5: Marginal kinetic distributions for the double well potential. Left: $\Delta t = 0.3$. Right: $\Delta t = 0.4$.

B.1.4 Verification of the first-order expansion

We verify the correctness first-order expansion of $\mu_{\Delta t, P}$ obtained in (B.19), by comparing the joint distributions obtained from Monte-Carlo simulations with a reference calculation of the first-order expansion for $\mu_{\Delta t, P}$. Additionally, we plot the empirical estimate of $\mu_{\Delta t, Q}$ and μ . The plots show joint likelihoods as a function of the state, using a color mapping. Empirical joint distributions for BAOA and BAOAB trajectories are plotted on the top row of each figure. On the bottom row, a reference computation of μ is plotted on the right, as well as a reference computation of

$$\left(1 + \frac{\Delta t}{2} g\right) \mu$$

on the left. The results visually confirm our result, while suggesting that, as a whole, $\mu_{\Delta t, Q}$ is the superior approximation of μ . See Figures B.6, B.7 and B.8.

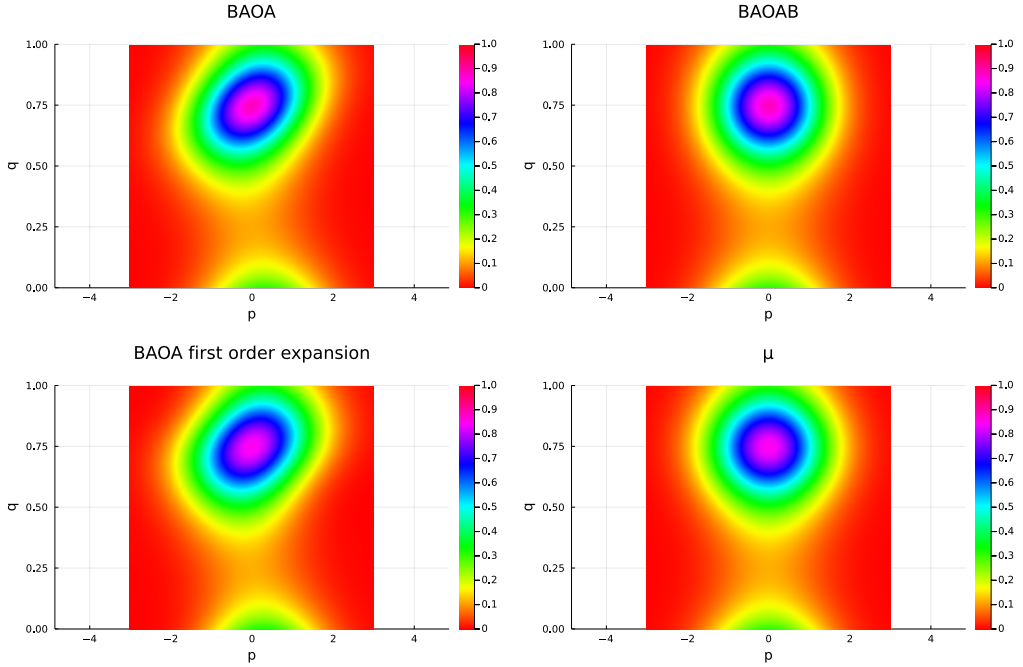


Figure B.6: Joint distributions for the periodic potential, $\Delta t = 0.1$.

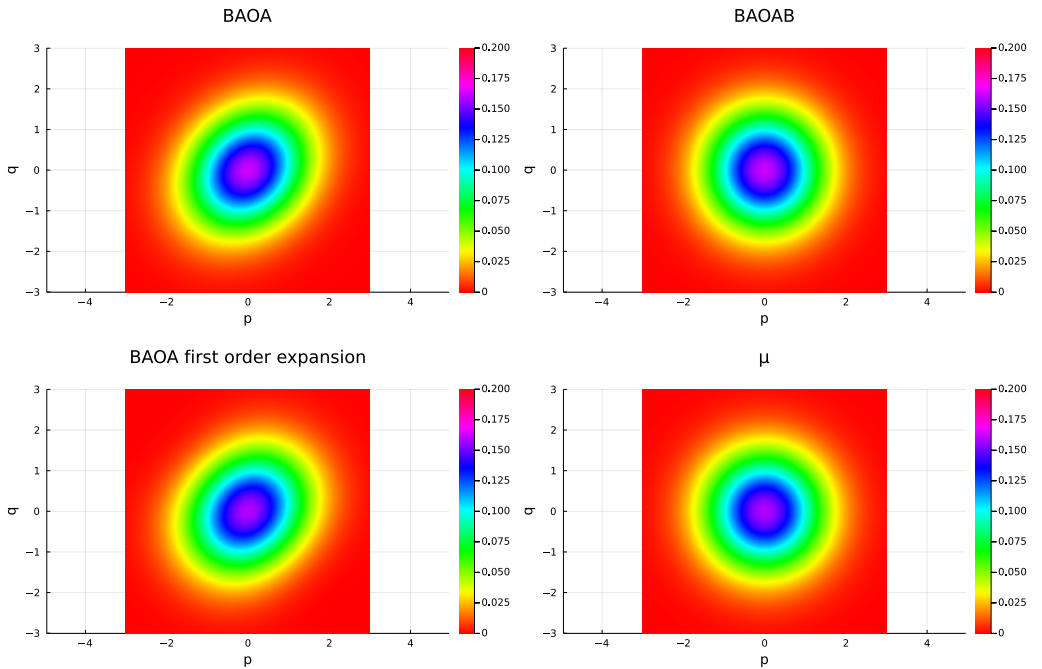


Figure B.7: Joint distributions for the quadratic potential, $\Delta t = 0.4$.

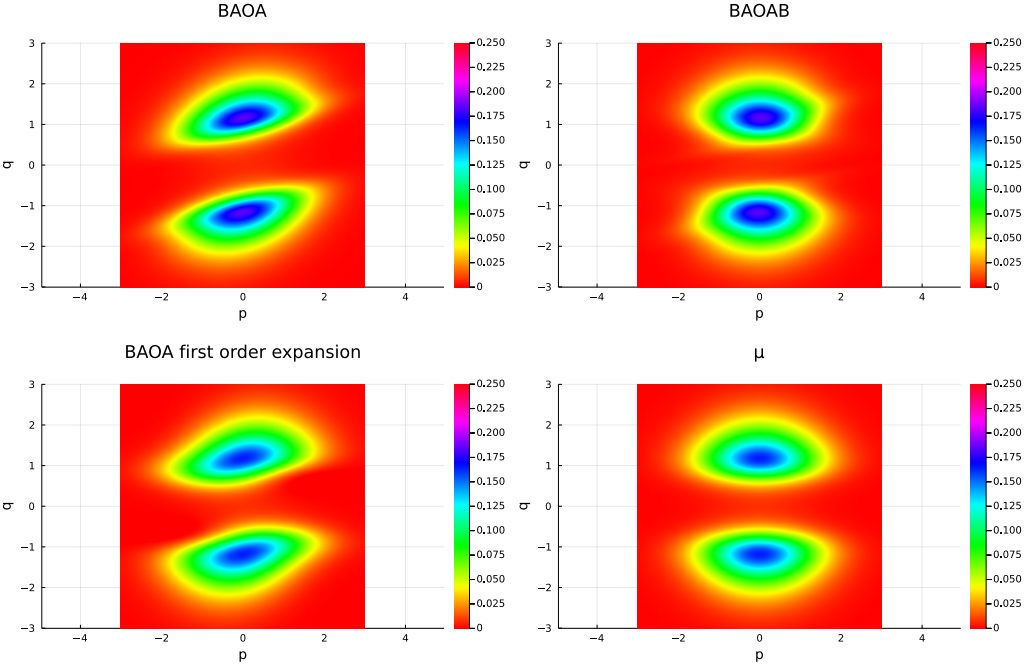


Figure B.8: Joint distributions for the double well potential, $\Delta t = 0.4$.

B.1.5 Example of first-order bias in a BAOA average

We demonstrate that for certain observables, BAOA is drastically outperformed by BAOAB, by calculating the average of g for increasing timesteps. Note by (B.21), the true average is 0. Figures B.9 and B.10 show the estimated averages as a function of the timestep on the left, and the same data on a log-log plot on the right. The order of the error on the BAOAB averages suggest that the second order error term

$$\int_{\mathcal{E}} g f_2 \, d\mu$$

given in (B.15) cancels out, yielding a fourth-order bias in Δt for BAOAB averages of g .

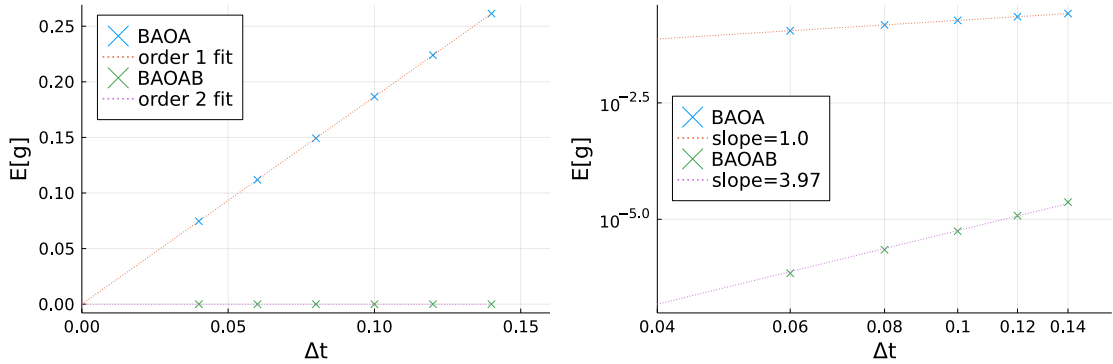


Figure B.9: Averages of g for the double well potential.

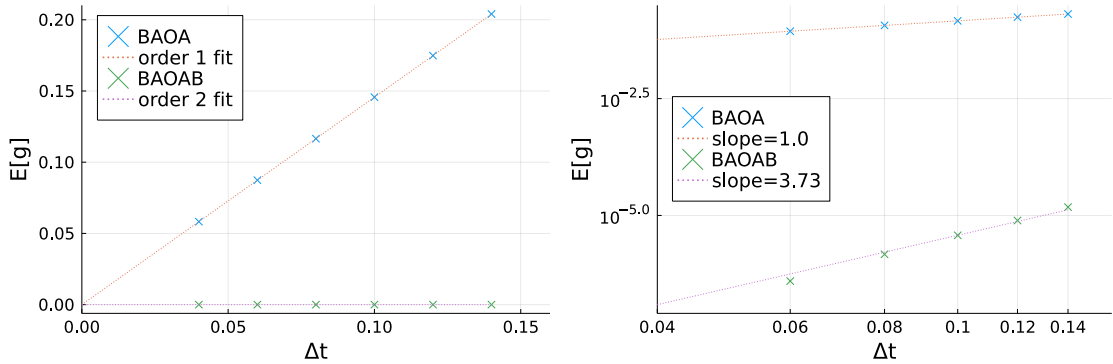


Figure B.10: Averages of g for the tilted double well potential.

B.1.6 Effect of the friction parameter

All experiments shown above used a value of $\gamma = 1$ for the friction parameter. In this final experiment, we examine the effect of changing γ . We show the marginal kinetic distributions for three values of $\gamma \in \{0.1, 1, 10\}$. The results show that there is no visually discernable effect of the parameter γ : all $\kappa_{\Delta t, P}$ s are superposed close to the reference curve, and all $\kappa_{\Delta t, Q}$ s are superposed above. This suggest that most of the error on $\kappa_{\Delta t, Q}$ arises from the additional term

$$-\frac{\Delta t^2}{8} \int_{\mathcal{E}} \varphi(A + B)g \, d\mu,$$

which is the dominant discrepancy term in (B.32), and which is independent of γ . This is the fact we observed numerically on figures B.5 and B.4. See figure B.11.

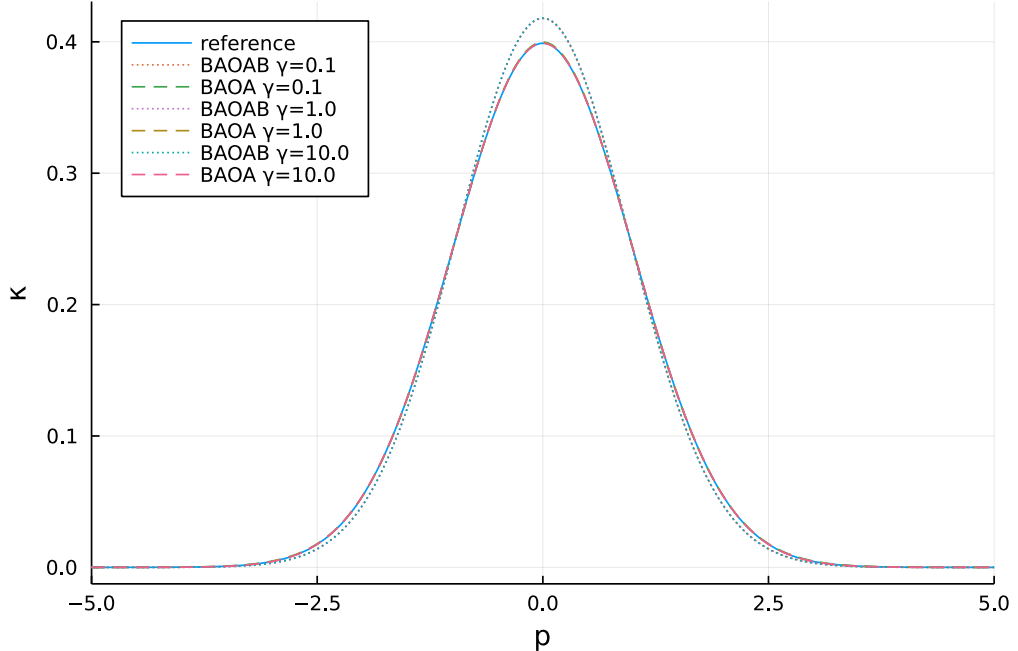


Figure B.11: Kinetic marginal distributions for $\Delta t = 0.3$ on the double well potential.

Appendix C

Notational conventions

Notational conventions

We convene that the gradient of a function $\varphi : \mathbb{R}^n \mapsto \mathbb{R}$ is a column vector-valued function

$$\nabla \varphi : \mathbb{R}^n \mapsto \mathbb{R}^n := \mathbb{R}^{n \times 1}$$

Notationally,

$$\nabla = \begin{pmatrix} \partial x_1 \\ \vdots \\ \partial x_n \end{pmatrix}$$

So that the Hessian operator writes

$$\nabla^2 := \nabla \nabla^\top = \begin{pmatrix} \partial x_1 \partial_{x_1} & \cdots & \partial x_1 \partial_{x_n} \\ \vdots & \ddots & \vdots \\ \partial x_n \partial_{x_1} & \cdots & \partial x_n \partial_{x_1} \end{pmatrix}$$

And for $f = (f_1, \dots, f_n)^\top : \mathbb{R}^n \mapsto \mathbb{R}^n$

$$(C.1) \quad \nabla f = \begin{pmatrix} \nabla^\top f_1 \\ \vdots \\ \nabla^\top f_n \end{pmatrix} = (\nabla \otimes f)^\top \quad \text{div } f = \partial_{x_1} f_1 + \cdots + \partial_{x_n} f_n = \nabla^\top f$$

are respectively the Jacobian matrix and divergence of f .

Bibliography

- [1] B. Leimkuhler, C. Matthews, G. Stoltz. The computation of averages from equilibrium and nonequilibrium Langevin molecular dynamics
<https://arxiv.org/abs/1308.5814v1>
- [2] S. Kieninger, B.G. Keller GROMACS Stochastic Dynamics and BAOAB are equivalent configurational sampling algorithms
<https://arxiv.org/abs/2204.02105>
- [3] E. Hairer, C. Lubich, G. Wanner, Geometric numerical integration illustrated by the Störmer-Verlet method, Acta Numerica 12 (2003) 399-450